Discovery of potent and broad-spectrum pyrazolopyridine-containing antivirals against enterovirus D68, A71, and coxsackievirus B3 by targeting the viral 2C protein

Yanmei Hu[†,‡], **Naoya Kitamura**[†,‡], **Rami Musharrafieh**[†], **Jun Wang**[*,†]

[†]Department of Pharmacology and Toxicology, College of Pharmacy, The University of Arizona, Tucson, Arizona 85721, United States

Abstract

The *enterovirus* genus of the picornavirus family contains many important human pathogens. EV-D68 primarily infects children, and the disease manifestations range from respiratory illnesses to neurological complications such as acute flaccid myelitis (AFM). EV-A71 is a major pathogen for the hand, foot, and mouth disease (HFMD) in children and can also lead to AFM and death in severe cases. CVB3 infection can cause cardiac arrhythmias, acute heart failure, as well as type 1 diabetes. There is currently no FDA-approved antiviral for any of these enteroviruses. In this study, we report our discovery and development of pyrazolopyridine-containing small molecules with potent and broad-spectrum antiviral activity against multiple strains of EV-D68, EV-A71, and CVB3. Serial viral passage experiments, coupled with reverse genetics and thermal shift binding assays, suggested that these molecules target the viral protein 2C. Overall, the pyrazolopyridine inhibitors represent a promising class of candidates for the urgently needed non-polio enterovirus antivirals.

Graphical Abstract

[*]**Corresponding Author Jun Wang** – Department of Pharmacology and toxicology, College of Pharmacy, University of Arizona, 1703 E. Mabel St, Tucson, AZ, 85721, United States; Phone: +1-520-626-1366; junwang@pharmacy.arizona.edu, Fax: 520-626-0749.
[‡]Y. M. and N. K. contributed equally.
Yanmei Hu – Department of Pharmacology and toxicology, College of Pharmacy, University of Arizona, 1703 E. Mabel St, Tucson, AZ, 85721, United States.
Naoya Kitamura – Department of Pharmacology and toxicology, College of Pharmacy, University of Arizona, 1703 E. Mabel St, Tucson, AZ, 85721, United States.
Rami Musharrafieh – Department of Pharmacology and toxicology, College of Pharmacy, University of Arizona, 1703 E. Mabel St, Tucson, AZ, 85721, United States.
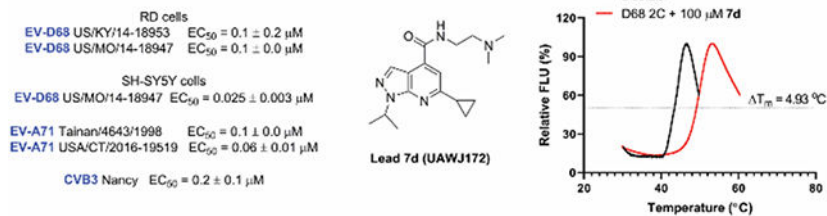
Supporting Information
The Supporting Information is available free of charge at
HPLC traces for the final products; Molecular Formula Strings.

INTRODUCTION

Enteroviruses such as enterovirus D68 (EV-D68), EV-A71, and coxsackievirus B3 (CVB3) are important human pathogens that have a significant impact on human health, especially in children.[1] EV-D68, EV-A71, CVB3, along with poliovirus and rhinovirus belong to the *Enterovirus* genera of the *Piconaviridae* virus family. Although poliovirus infection was nearly eliminated by the Global Polio Eradication Initiative through effective vaccination, no vaccines are available in the United States for the non-polio enteroviruses such as EV-D68, EV-A71, and CVB3. Three inactivated EV-A71 vaccines are available in China.[2-4] However, their efficacy is limited to certain strains and are not broadly protective.[5] Therefore, it is imperative to develop small molecule antivirals as therapeutics.[5-8] Drug discovery efforts on non-polio enterovirus antivirals gained momentum in recent years due to the increasing number of infections and severity of the disease outcomes caused by EV-D68, EV-A71, and CVB3.[9-11] EV-D68 infection typically leads to moderate flu-like respiratory illness and it is self-limiting.[12, 13] EV-D68 spreads through the respiratory tract, similar to rhinoviruses. However, contemporary EV-D68 strains appear to evolve and become more virulent compared to historic strains.[14] For example, recent EV-D68 outbreaks in 2014, 2016, and 2018 coincided with increasing numbers of severe respiratory illness and neurological complications such as acute flaccid myelitis (AFM), meningitis, and encephalitis.[13, 15-18] It has been shown in cell culture that contemporary EV-D68 strains, but not historic strains, were able to infect neuronal cells and cause cytopathic effect.[14] In studies carried out using a mouse model, EV-D68 virus was shown to infiltrate the blood brain barrier and infect the central nervous system (CNS) such as the spinal cord.[19-23] Although EV-D68 virus is rarely detected in the human patient CNS tissues, there is nevertheless a positive correlation between EV-D68 infection and neurological complications as shown by a number of studies.[24, 25] Recent studies have shown that antibodies reacting to the EV-D68 viral capsid protein VP1 have been detected in high frequency in the CSF fluid samples from AFM patients.[25] EV-A71 is one of the etiological agents for hand, foot, and mouth disease (HFMD) and spreads through the fecal-oral route. Several EV-A71 outbreaks in the Asia-Pacific region have resulted in thousands of deaths.[5] Similar to EV-D68, EV-A71 is also a neurotropic virus, and in rare cases EV-A71 infection can cause severe neurological complications with a high mortality and morbidity rate in infants and young children.[26, 27] CVB3 virus is the causative agent for viral myocarditis.[28] In addition, CVB3 infection is

also linked to type 1 diabetes mellitus and idiopathic chronic pancreatitis due to chronic pancreatic inflammation induced by the virus.[29]

Several compounds have been reported in the literature as non-polio antivirals with varying degrees of potency, selectivity index, and antiviral spectrum.[1, 5, 7, 30] Prominent examples include viral capsid inhibitors such as pleconaril, the viral protease inhibitor rupintrivir, the 3D polymerase inhibitors ribavirin and gemcitabine, as well as the viral 2C inhibitors dibucaine and fluoxetine.[31-36] Most of these reported compounds are either repurposed from rhinovirus antivirals (pleconaril and rupintrivir) or FDA-approved drugs for other disease indications (fluoxetine, dibucaine, and ribavirin).[31] As these compounds were not specifically developed for EV-D68, EV-A71 or CVB3, their antiviral specificity, potency, and selectivity index need to be significantly improved for clinical use as non-polio enterovirus antivirals. Notably, EV-D68 antiviral development is left far behind compared to EV-A71 and CVB3,[7] possibly because it is an emerging pathogen that only comes to public attention in recent years.[37] Our primary interest is therefore to develop broad-acting non-polio enterovirus antivirals against EV-D68, EV-A71, and CVB3.

In this study, we have identified a class of pyrazolopyridine analogs that have shown broad-spectrum antiviral activity against EV-D68, EV-A71, and CVB3. The primary hit, compound **7a**, was identified through a cytopathic effect (CPE) assay screening against EV-D68 virus.[38, 39] Encouragingly, compound **7a** was also active against EV-A71. Subsequent structure-activity relationship (SAR) studies yielded several lead compounds including **7d** that inhibited different strains of EV-D68, EV-A71 and CVB3 with EC_{50} values in the nanomolar range and a cellular selectivity index of over 500. The antiviral activity was also consistent between the RD cell (muscle cell) and the SH-SY5Y cell (neuronal cell). Mechanistic studies have shown that the pyrazolopyridine analogs target the conserved viral 2C protein. The EV-A71 2C protein was proposed to form a hexamer according to the X-ray crystal structure, and has been shown to have ATPase activity and helicase acctivity.[40, 41] Additional recognized functions of 2C include viral RNA binding and replication, membrane remodeling, and encapsidation.[42] Structurally diverse compounds have been identified as 2C inhibitors (Figure 1).[30-33, 35, 36, 38] The pyrazolopyridine compounds discovered in this study represent one of the most potent classes of compounds with broad-spectrum antiviral activity against non-polio enteroviruses reported so far.

RESULTS AND DISCOSSION

Chemistry

The synthesis of 1*H*-pyrazolo[3,4,-*b*]pyridine-4-carboxylic acid **4** followed the previously reported procedures (Figure 2A).[30, 43] Briefly, condensation of 1-alkylpyrazole-5-amine or 1,3-dialkylpyrazole-5-amine **1** with the 4-alkyl-2,4-diketoester **2** in the presence of acetic acid gave the 1*H*-pyrazolo[3,4,-*b*]pyridine-4-carboxylic ester intermediate **3**. Subsequent hydrolysis using potassium hydroxide in isopropanol gave the key intermediate 1*H*-pyrazolo[3,4,-*b*]pyridine-4-carboxylic acid **4**. Next, for final compounds that contain tertiary amine (**7g** as an example), a one-step HATU-mediated amide coupling was used (Figure 2B). For final compounds that contain either primary amine or secondary amine (**7k** as an example), a two-step process was applied: the first step was HATU-mediated amide coupling

with the mono-Boc-protected diamine, and this was followed by TFA deprotection to give the final product (Figure 2B).

Structure-activity relationship studies

The initial hit compound **7a** was identified as an EV-D68 antiviral through a CPE-based phenotypic screening of the Enamine compound library.[38, 39] It inhibited the contemporary EV-D68 US/KY/14-18953 strain with an EC_{50} value of 16.7 μM and a selectivity index of 10.6 (Table 1). Gratifyingly, compound **7a** also inhibited the closely related EV-A71 (Tainan/4643/1998) virus with an EC_{50} value of 8.1 μM. To further optimize the antiviral potency, selectivity index, and spectrum of antiviral activity of **7a**, we subsequently initiated a structure-activity relationship study. Specifically, we focused on diversifying the 1-alkyl R_1, 3-alkyl R_3, 4-amide R_4, and 6-alkyl R_6 substitutions on the 1H-pyrazolo[3,4,-b]pyridine core (Figure 2B).

For the initial screening, all compounds were titrated to determine the antiviral efficacy and cellular cytotoxicity in viral CPE assay and neutral red uptake cell viability assay, respectively. Human rhabdomyosarcoma (RD) cells were used for EV-D68 and EV-A71 antiviral assays, and Vero cells were used for the CVB3 antiviral assay. For the CPE assay, virus-infected cells were treated with serial dilutions of compounds for 3 days, and cell viability were determined by neutral red uptake assay. For compound **7** series with 1-isoproyl and 6-cyclopropyl substitutions (**7a–7m**), it was found that the 4-position amide substitution had a profound effect on the antiviral activity and selectivity index (Table 1). Replacing the neutral ester in **7a** with pyrrolidine gave compound **7b**, which had significantly improved antiviral efficacy. Compound **7c** with diethylamine also had submicromolar EC_{50} values against all three viruses. Changing diethylamine to dimethylamine gave compound **7d**, which had increased selectivity index. Compound **7e** with a shorter linker between the amide and the terminal amine was less active (**7e** vs **7d**). Compound **7g** with a cyclized liker was highly potent (EC_{50} = 0.02 μM) but was less selective than **7f** as shown by its low CC_{50} values (CC_{50} = 20.7 μM and 33.8 μM in RD and Vero cells, respectively). Compounds containing secondary or primary amine were less potent as the compounds containing tertiary amine (**7h, 7i** vs **7d**, and **7j** vs **7f**). Extending the linker between the amide and terminal amine from ethyl to propyl gave compounds **7k, 7l**, and **7m**, which had reduced antiviral activity compared with corresponding compounds with the ethyl linker (**7k** vs **7c, 7l** vs **7d, 7m** vs **7h**). Overall, the most potent and selective compound from compound 7 series were **7b, 7d, 7f, 7g**, and **7h**, which had more than 100-fold improvement in antiviral efficacy compared to the original hit **7a** against EV-D68 virus.

For compound **10** series (**10a–10f**) with 6-isopropyl substitution, we selected the favorable amide substitutions from compound **7** series, and compounds **10a, 10c–10f** turned out to have high antiviral potency and selectivity index (EC_{50} < 1 μM and SI_{50} > 120). Compounds **10b** with a neutral terminal hydroxyl group had drastically reduced antiviral activity (EC_{50} = 9.8 μM) against EV-D68, which is similar to antiviral activity of the screening hit **7a**. These results suggest that the terminal positive charge is critical for the potent antiviral activity. The most potent and selective compound from this series was compound **10a**.

Compounds with 6-tert-butyl substitution **11a** and **11b** also had potent antiviral efficacy but the selectivity index was lower compared to compounds with 6-isopropyl substitution (**11a** vs **10a**, and **11b** vs **10e**). Compounds with 6-methyl substitution **12a–12e, 13, 14**, and **15a– 15b** were generally less active, except compound **12a**. Next, the 1-position substitution was examined. Compound **16** with 1-ethyl substitution was less active than the analog **7d** with 1-isopropyl substation. Nevertheless, the EC_{50} values were still at the single-digit micromolar range across three different viruses. Compound **17** with 1-methyl substitution was less active, showing an EC_{50} value of 9.8 μM against the EV-D68 virus. Compounds **18a** and **18b** with 1-tert-butyl and 3-methyl substitutions also had potent antiviral activity but with low CC_{50} values. Compound **19** had similar antiviral activity as compound **18a** against EV-D68 but had a higher selectivity index. Compound **20** with 1-propyl substitution, compound **21** with 1-isobutyl substitution, and compound **22** with 1-cyclopropylethyl substitution all had low single-digit or submicromolar EC_{50} values against all three viruses, but their cellular cytotoxicity was higher than compound **7d**, which had 1-isopropyl substitution.

It is noted that an earlier study similarly reported the pyrazolopyridine derivatives such as **JX040** (Table 1 last row) as antiviral drugs specific for enteroviruses.[30] Those compounds had antiviral activity against EV-A71, CVB3, and poliovirus-1, but their antiviral activity was not tested against the EV-D68. Our study showed that **JX040** also had potent antiviral activity against two EV-D68 strains US/KY/14-18953 and US/MO/14-18947 with EC_{50} values of 0.2 μM and 0.1 μM, respectively. An earlier study from the same group showed that similar compounds inhibited the CVB3 virus by targeting the viral 2C protein.[35] Although the compounds described in our study such as **7d** share the same pyrazolopyridine core with the ones reported earlier such as **JX040**, the structure-activity relationships appear to be different. For example, compounds in the earlier study such as **JX040** had aromatic amide substitutions at the 4-position, while compounds from our study such as **7d** prefer positively charged amine with a hydrophobic alkyl linker at the same position. In addition, compounds reported earlier had aromatic substitutions at the 6-position, while our compounds contain hydrophobic alkyl substitutions. Given that both subtypes of compounds showed broad-spectrum antiviral activity against non-polio enteroviruses, further structural studies are needed to delineate their binding sites in the 2C protein.

Summary of structure-activity relationship

The summary of the SAR results was shown in Figure 3. For position 1 substitution, branched alkyl substitutions such as isopropyl, tert-butyl, isobutyl, and 1-cyclopropylethyl were favored over methyl, ethyl, propyl, and cyclopentyl, and compounds with 1-isobutyl and 1-(1-cyclopropylehtyl) substitution had a lower selectivity index (highlighted in red). For position 3 substitution, both methyl and hydrogen were tolerated. For the 4-position amide, the ethyl linker was preferred over the propyl linker. The terminal amine could be tertiary, secondary or primary amine. For the 6-position substitution, both small and bulky alkyl substitutions were tolerated, and tert-butyl substitution led to lower selectivity index (highlighted in red).

Broad-spectrum antiviral activity

Encouraged by the potent and broad-spectrum antiviral activity of these pyrazolopyridine analogs, we selected four lead candidates **7d, 7h, 10a**, and **19** with the highest potency and selectivity index from the primary screening, and tested their antiviral activity against several other contemporary EV-D68 and EV-A71 strains (Table 2). The EV-D68 strains selected were from the 2014 outbreak and have been linked with AFM.[14] Compound **7d** is the most potent lead compound with EC_{50} values ranging from 0.04 to 0.1 μM against all EV-D68 and EV-A71 strains tested as well as a high selectivity index of over 2000. Compounds **7h** and **10a** had similar antiviral activity against different strains of EV-D68 and EV-A71 with EC_{50} values ranging from 0.06 to 0.3 μM and a selectivity index of over 700. Compound **19** was less active compared to **7d, 7h**, and **10a**, but it remains a potent inhibitor with broad-acting activity against all strains tested (EC_{50} = 0.4 to 7.4 μM; SI_{50} > 100). Overall, consistent antiviral efficacy was observed across different strains of EV-D68 and EV-A71, suggesting these pyrazolopyridine compounds might target a conserved viral protein among enteroviruses or a common host signaling pathway that is essential for the viral replication.

Antiviral activity in secondary plaque assay

The antiviral activity of compounds **7d, 7h, 10a**, and **19** against EV-D68 US/MO/14-18947 were further confirmed in the secondary plaque assay (Figure 4). Telaprevir, an EV-D68 2A protease inhibitor,[44] was included as a positive control and showed complete inhibition of plaque formation at 3 μM. All four compounds showed dose dependent inhibition of plaque formation and the EC_{50} values for **7d, 7h, 10a**, and **19** were 0.025, 0.077, 0.023, and 0.13 μM, respectively. These results were consistent with the primary CPE assay results shown in Table 2.

Antiviral activity against EV-D68 in neuronal cells

As contemporary EV-D68 viruses are neurotropic, we are interested in testing whether the pyrazolopyridine compounds can inhibit EV-D68 virus replication in neuronal cells. For this, four lead compounds **7d, 7h, 10a**, and **19** were tested against the neurotropic EV-D68 strain US/MO/14-18947 in neuronal cell line SH-SY5Y (Figure 5). Viral replication was quantified by immunofluorescence staining using anti-VP1 antibody. Pleconaril was included as a positive control. Pleconaril is a known viral capsid protein VP1 inhibitor and has potent antiviral activity against multiple EV-D68 strains. As shown in Figure 5, pleconaril completely abolished viral replication at 50 μM as shown by the lack of VP1 fluorescence signal. All four compounds **7d, 7h, 10a**, and **19** inhibited viral replication in a dose-response manner with EC_{50} values of 0.03, 0.07, 0.03, and 0.34 μM, respectively, which is consistent with their antiviral efficacy in RD cells (Table 2). In summary, all four pyrazolopyridine compounds potently inhibit the neurotropic EV-D68 virus replication in neuronal cells.

Mechanism of action

To delineate the mechanism of action of these pyrazolopyridine analogs, we first attempted to select drug-resistant mutant viruses through serial viral passage experiments. For this,

we chose compound **7d** as a chemical probe and the EV-D68 US/MO/14-18947 virus as a representative non-polio enterovirus. Compound **7d** inhibited EV-D68 US/MO/14-18947 virus with an EC_{50} value of 0.07 ± 0.02 μM in CPE assay. EV-D68 US/MO/14-18947 virus was amplified in RD cells with escalating drug selection pressure, starting from ~1×EC_{50} at passages 1 and 2, and increased to 2×EC_{50}, 4×EC_{50}, and 8×EC_{50} at passages 3, 4, and 5, respectively (Table 3). The drug sensitivity of passage 5 (P5) virus was tested against compound **7d** in CPE assay. The EC_{50} of compound **7d** against P5 virus was 1.9 ± 0.2 μM, a 27-fold increase compared to P0 virus, suggesting resistance might have emerged. We then sequenced the whole viral genome and identified two mutations in the viral 2C protein, D183V and D323G. To validate the resistance phenotype, we generated recombinant viruses that harbor these 2C mutations and test their drug sensitivity against compound **7d**.[38, 44] Because P5 virus was sequenced as a mixture, it was unknown whether these two mutations emerged from the same virus or different viruses. As such, we generated three mutant recombinant viruses, the single mutant EV-D68/2C-D183V (rD183V) and EV-D68/2C-D323G (rD323G) viruses, and the double-mutant EV-D68/2C-D183V+D183V (rD183V/D323G) virus using the reverse genetics system we developed earlier.[38, 44] In brief, we introduced 2C-D183V, 2C-D323G, or 2C-D183V+D323G into the EV-D68 US/MO/14-18947 genome individually via a reverse genetics approach using a pHH21 vector. The recombinant WT virus (rWT) was also generated for comparison.

To determine which recombinant virus(s) confers the phenotypic drug resistance, we titrated **7d** against these viruses in the plaque assay (Figure 6A). It was found that the drug sensitivity of **7d** against rD183V virus was decreased by 22-fold compared to rWT virus (rD183V $EC_{50} = 0.66$ μM vs rWT $EC_{50} = 0.03$ μM), suggesting the 2C-D183V is the predominant drug resistant mutant. In contrast, the 2C-D323G only conferred moderate drug resistance and the drug sensitivity of **7d** against rD323G virus was decreased by 3-fold (rD323G $EC_{50} = 0.09$ μM vs rWT $EC_{50} = 0.03$ μM). The double mutant virus rD183V/D323G had more profound resistance and decreased the drug sensitivity by 33-fold (rD183V/D323G $EC_{50} = 1.00$ μM vs rWT $EC_{50} = 0.03$ μM). These results suggest that viral 2C protein might be the drug target of **7d**, and 2C-D183V mutant and to a less extent 2C-D323G mutant confer the phenotypic drug resistance in cell culture.

To further confirm that viral 2C protein is the direct drug target of **7d**, we performed the differential scanning calorimetry (DSC) assay,[45-48] also called thermal shift assay, to characterize the direct binding of **7d** to 2C protein and its mutants (Figure 6B). For this, we expressed the EV-D68 US/MO/14-18947 2C protein as well as the 2C-D183V, 2C-D323G, and 2C-D183V/D323G mutants. Binding of **7d** to WT 2C protein is evident as shown by stabilization of the protein by 4.93 °C in T_m shift (Figure 6B). In contrast, no binding was observed for the 2C-D183V mutant ($T_m = 0.01$ °C). The 2C-D323G mutant can also be stabilized by **7d** and the T_m was 3.92 °C, which is comparable to that of the WT 2C protein. The 2C-D183V/D323G double mutant had drastically reduced binding to **7d** compared to WT 2C ($T_m = 0.61$ °C vs 4.93 °C) (Table 5B). Consistent with CPE assay results described above for recombinant EV-D68 viruses (Figure 6A), the DSC assay results showed that the 2C-D183V is the predominant drug resistant mutant, while the

2C-D323G only confers moderate drug resistance, and combination of these two mutants further increased the degree of drug resistance.

As compound **7d** and its analogs have broad-spectrum antiviral activity against EV-A71 and CVB3 in addition to EV-D68, we further expressed the EV-A71 and CVB3 2C protein and performed DSC assay to confirm the direct binding of **7d** to these 2C proteins (Figure 6C). As expected, **7d** showed dose-dependent binding to EV-A71 and CVB3 2C proteins, similar to EV-D68 2C (Figure 6D). This result implies that **7d** inhibits EV-A71 and CVB3 by similarly targeting their viral 2C proteins.

The drug-resistant rD183V/D323G virus had a reduced fitness of replication compared to WT virus

To profile the fitness of replication of the rD183V/D323G virus, we conducted viral competition growth assay with the rWT virus. In the viral competition assay, the rWT and rD183V/D323G viruses were mixed at a 1:100 ratio at passage 0 to favor the mutant virus, and the mixture was co-cultured in RD cells for several passages. At each passage, the viral 2C protein was sequenced to determine the relevant ratios of the substitutions at residues 183 and 323. It was found that the rWT completely overtook the rD183V/D323G mutant virus at passage 3 (Figure 7A). To rule out the possibility that the rD183V/D323G virus might revert to WT by itself without the selection pressure, we passaged rD183V/D323G virus alone four times and found no change on the viral 2C protein (Figure 7B), suggesting the mutant virus is stable in the absence of competition from WT virus. Taken together, these results suggest that rD183V/D323G virus had a reduced fitness of replication compared to rWT.

CONCLUSIONS

Non-polio enteroviruses are important human pathogens and present a challenge for public health, especially in children and immunocompromised adults. Therefore, there is a dire need to develop effect antivirals targeting non-polio enteroviruses including EV-D68, EV-A71, and CVB3. In this study, we report our discovery of a series of pyrazolopyridine compounds with potent and broad-spectrum antiviral activity against non-polio enteroviruses. Starting from a screening hit **7a**, we conducted structure-activity relationship studies, which yielded several lead compounds including **7d, 7h, 10a**, and **19** with significant improved antiviral activity and cellular selectivity. The mechanism of action was delineated through resistance selection using compound **7d** as a chemical probe and the EV-D68 US/MO/14-18947 virus as a representative non-polio enterovirus. Two mutations at the viral 2C protein were identified, 2C-D183V and 2C-D323G. Using the reverse genetics system we developed earlier, we generated the recombinant EV-D68 viruses with either single or double 2C mutants selected from the passage experiment. It was found that the D183V is the dominant drug resistant mutant, while D323G only confers moderate resistance. This was further supported by the thermal shift assay results. In addition, we have shown that compound **7d** similarly binds to EV-A71 and CVB3 2C protein, implying that its antiviral activity against EV-A71 and CVB3 was through targeting the viral 2C proteins. Although resistance could be isolated in cell culture against **7d**, it was found that rD183V/

D323G mutant virus had reduced fitness of replication compared with WT as shown by the competition growth assay results (Figure 7).

Despite a number of 2C protein inhibitors being developed including the ones described here, the high-resolution X-ray crystal structure of the EV-D68 2C protein has not been solved. It is critical to obtain the drug bound complexes of 2C with different inhibitors, which will greatly facilitate the rational drug design. To our knowledge, the compounds reported herein represent the most potent antivirals against non-polio enteroviruses with a high cellular selectivity index. Further optimization might yield drug candidates for *in vivo* animal model studies as well as chemical probes for *in vivo* drug target validation.

EXPERIMENTAL SECTION

General chemical methods.

All chemicals were purchased from commercial vendors and used without further purification unless otherwise noted. ^{1}H and ^{13}C NMR spectra were recorded on a Bruker-400 or −500 NMR spectrometer. Chemical shifts are reported in parts per million referenced with respect to residual solvent (CD$_3$OD) 3.31 ppm, (DMSO-d6) 2.50 ppm, and (CDCl$_3$) 7.26 ppm or from internal standard tetramethylsilane (TMS) 0.00 ppm. The following abbreviations were used in reporting spectra: s, singlet; d, doublet; t, triplet; q, quartet; m, multiplet; dd, doublet of doublets; ddd, doublet of doublet of doublets. All reactions were carried out under N$_2$ atmosphere, unless otherwise stated. HPLC-grade solvents were used for all reactions. Flash column chromatography was performed using silica gel (230–400 mesh, Merck). High resolution mass spectra were obtained using an OrbitrapTM for all the compounds, obtained in an Ion Cyclotron Resonance (ICR) spectrometer. The purity was assessed by using Shimadzu UPLC with Shimdazu C18-AQ column (4.6x150 mm P/N #227-30767-05) at a flow rate of 1 mL/min; λ = 254 and 220 nm; mobile phase A, 0.1% trifluoroacetic acid in H$_2$O, and mobile phase B, 0.1% trifluoroacetic acid in 90% CH$_3$CN and 10% H$_2$O. The gradients are 0-2 mins 10% B, 2-15mins 10%-100% B, 15-18mins, 100% B, 18.1-20mins 10% B. All compounds submitted for testing were confirmed to be > 95.0% purity by HPLC traces. All final products were characterized by proton and carbon NMR, HPLC and ESI-MS.

Synthesis procedures

General procedure for the synthesis of 1H-pyrazolo[3,4-b]pyridine-4-carboxylic ester intermediate 3.—The 1-alkylpyrazole-5-amine or the 1,3-dialkylpyrazole-5-amine (1 mmol) and the 4-alkyl-2,4-diketoester (1mmol) was dissolved in acetic acid (10 ml). The resulting solution was refluxed for 5 h under a nitrogen atmosphere. After cooling down to ambient temperature, the solvent was removed in vacuo and the resulting residue was purified by silica gel flash column chromatography (10-50% ethyl acetate/hexane) to give the final product.

General procedure for the synthesis of 1H-pyrazolo[3,4-b]pyridine-4-carboxylic acid intermediate 4.—The ester **3** (1 mmol) was dissolved in isopropanol (5 ml). Potassium hydroxide (2 mmol) was added in on portion and the resulting solution

was stirred at ambient temperature until complete disappearance of the starting material as monitored by TLC (2 to 4h). Solvent was removed in vacuo and the resulting residue was extracted with dichloromethane and 3 N HCl. The organic layer was dried over $MgSO_4$, filtered, and concentrated under reduced pressure. The crude product was purified by flash column chromatography (1-10% CH_3OH/CH_2Cl_2) to give the final product.

General procedure of amide coupling.—To a DMF solution of carboxylic acid (1 mmol) was added HATU (1 mmol) and DIEA (1.2 mmol). After stirring for 2 minutes, amine (1 mmol) was added. The resulting solution was stirred overnight at ambient temperature. The reaction was diluted with dichloromethane and extracted with aqueous $NaHCO_3$ solution, followed by brine. The organic layer was dried over $MgSO_4$, filtered, and concentrated under reduced pressure. The crude product was purified by flash column chromatography (1-10% CH_3OH/CH_2Cl_2) to give the final product.

General procedure of TFA deprotection of Boc.—The Boc-protected amide intermediate (1mmol) was dissolved in dichloromethane (5 ml), and TFA (2 ml) was added cautiously. The resulting mixture was stirred at ambient temperature for 5 h, and then the solvent was removed and the final product was purified by flash column chromatography (1-10% CH_3OH/CH_2Cl_2).

The following compounds were synthesized using the same procedure as shown for compound **7g: 7a, 7b, 7c, 7d, 7f, 7g, 7k, 7l, 10a, 10b, 10c, 11a, 12a, 12b, 12c, 13, 14, 15a, 16, 17, 18a, 19, 20, 21, 22**, and **JX040**.

The following compounds were synthesized using the same procedure as shown for compound **7k: 7e, 7h, 7i, 7j, 7m, 10d, 10e, 10f, 11b, 12d, 12e, 15b**, and **18b**.

Compound Characterization

6-cyclopropyl-1-(propan-2-yl)-1H-pyrazolo[3,4-b]pyridine-4-carboxylic acid (4a).—Yield: 35%. ^{1}H NMR (400 MHz, DMSO-d_6) δ 13.73 (brs, 1H), 8.22 (s, 1H), 7.59 (s, 1H), 5.22 – 5.02 (m, 1H), 2.44 – 2.27 (m, 1H), 1.47 (d, J = 6.7 Hz, 6H), 1.15 – 0.98 (m, 4H). ^{13}C NMR (101 MHz, DMSO-d_6) δ 166.3, 162.9, 150.2, 131.7, 131.6, 116.3, 111.1, 48.2, 21.8, 17.1, 11.1. $C_{13}H_{15}N_3O_2$, EI-MS: m/z (M-H^{+}): 244.3 (calculated), 244.3 (found).

1,6-bis(propan-2-yl)-1H-pyrazolo[3,4-b]pyridine-4-carboxylic acid (4b).—Yield: 22%. ^{1}H NMR (400 MHz, DMSO-d_6) δ 13.75 (s, 1H), 8.27 (s, 1H), 7.60 (s, 1H), 5.33 – 5.11 (m, 1H), 3.35 – 3.12 (m, 1H), 1.50 (d, J = 6.7 Hz, 7H), 1.31 (d, J = 6.9 Hz, 7H). ^{13}C NMR (101 MHz, DMSO-d_6) δ 166.7, 166.3, 149.9, 132.2, 131.6, 115.7, 111.3, 48.2, 35.8, 22.4, 21.9. $C_{13}H_{17}N_3O_2$, EI-MS: m/z (M-H^{+}): 246.3 (calculated), 246.3 (found).

6-tert-butyl-1-(propan-2-yl)-1H-pyrazolo[3,4-b]pyridine-4-carboxylic acid (4c).—Yield: 31%. ^{1}H NMR (400 MHz, DMSO-d_6) δ 8.26 (s, 1H), 7.75 (s, 1H), 5.33 – 5.08 (m, 1H), 1.52 (d, J = 6.7 Hz, 6H), 1.41 (s, 9H). ^{13}C NMR (101 MHz, DMSO-d_6) δ 168.4, 166.3, 149.4, 132.2, 131.3, 113.7, 110.9, 48.5, 37.8, 29.9, 21.7. $C_{14}H_{19}N_3O_2$, EI-MS: m/z (M-H^{+}): 260.3 (calculated), 260.3 (found).

6-methyl-1-(propan-2-yl)-1H-pyrazolo[3,4-b]pyridine-4-carboxylic acid (4d).—
Yield: 27%. ^{1}H NMR (400 MHz, DMSO-d_6) δ 13.75 (brs, 1H), 8.26 (s, 1H), 7.55 (s, 1H), 5.39 – 5.09 (m, 1H), 2.67 (s, 3H), 1.48 (d, J = 6.7 Hz, 6H). ^{13}C NMR (101 MHz, DMSO-d_6) δ 166.2, 158.1, 149.9, 131.7, 131.6, 117.9, 110.8, 47.8, 24.4, 21.9. $C_{11}H_{13}N_3O_2$, EI-MS: m/z (M-H$^+$): 218.2 (calculated), 218.3 (found).

1-cyclopentyl-6-methyl-1H-pyrazolo[3,4-b]pyridine-4-carboxylic acid (4e).—
Yield: 41%. ^{1}H NMR (400 MHz, DMSO-d_6) δ 8.26 (s, 1H), 7.55 (s, 1H), 5.47 – 5.29 (m, 1H), 2.67 (s, 3H), 2.18 – 2.06 (m, 2H), 2.06 – 1.78 (m, 4H), 1.78 – 1.60 (m, 2H). ^{13}C NMR (101 MHz, DMSO-d_6) δ 166.2, 158.2, 150.5, 132.0, 131.7, 117.9, 110.8, 56.6, 32.0, 24.4, 24.2. $C_{13}H_{15}N_3O_2$, EI-MS: m/z (M-H$^+$): 244.3 (calculated), 244.3 (found).

6-methyl-1-propyl-1H-pyrazolo[3,4-b]pyridine-4-carboxylic acid (4f).—Yield:
38%. ^{1}H NMR (400 MHz, DMSO-d_6) δ 13.76 (brs, 1H), 8.25 (s, 1H), 7.55 (s, 1H), 4.40 (t, J = 7.0 Hz, 2H), 2.66 (s, 3H), 2.01 – 1.75 (m, 2H), 0.82 (t, J = 7.4 Hz, 3H). ^{13}C NMR (101 MHz, DMSO-d_6) δ 166.1, 158.4, 150.8, 131.8, 131.7, 117.8, 110.6, 47.9, 24.4, 22.5, 11.0. $C_{11}H_{13}N_3O_2$, EI-MS: m/z (M-H$^+$): 218.2 (calculated), 218.2 (found).

1-ethyl-6-methyl-1H-pyrazolo[3,4-b]pyridine-4-carboxylic acid (4g).—Yield: 27%.
^{1}H NMR (400 MHz, DMSO-d_6) δ 13.77 (brs, 1H), 8.25 (s, 1H), 7.55 (s, 1H), 4.48 (q, J = 7.2 Hz, 2H), 2.67 (s, 3H), 1.42 (t, J = 7.2 Hz, 3H). ^{13}C NMR (101 MHz, DMSO-d_6) δ 166.1, 158.4, 150.3, 131.8, 131.7, 117.8, 110.7, 41.4, 24.4, 14.7. $C_{10}H_{11}N_3O_2$, EI-MS: m/z (M-H$^+$): 204.2 (calculated), 204.2 (found).

6-cyclopropyl-1-ethyl-1H-pyrazolo[3,4-b]pyridine-4-carboxylic acid (4h).—Yield:
36%. ^{1}H NMR (400 MHz, DMSO-d_6) δ 13.78 (brs, 1H), 8.21 (s, 1H), 7.59 (s, 1H), 4.42 (q, J = 7.2 Hz, 2H), 2.44 – 2.27 (m, 1H), 1.40 (t, J = 7.2 Hz, 3H), 1.19 – 0.98 (m, 4H). ^{13}C NMR (101 MHz, DMSO-d_6) δ 166.2, 163.1, 150.4, 131.7, 131.6, 116.2, 110.8, 41.4, 17.1, 14.6, 11.0. $C_{12}H_{13}N_3O_2$, EI-MS: m/z (M-H$^+$): 230.3 (calculated), 230.2 (found).

6-cyclopropyl-1-methyl-1H-pyrazolo[3,4-b]pyridine-4-carboxylic acid (4i).—
Yield: 22%. ^{1}H NMR (400 MHz, DMSO-d_6) δ 13.80 (brs, 1H), 8.21 (s, 1H), 7.60 (s, 1H), 4.00 (s, 3H), 2.44 – 2.32 (m, 1H), 1.18 – 1.00 (m, 4H). ^{13}C NMR (101 MHz, DMSO-d_6) δ 166.15, 163.23, 150.96, 131.68, 131.62, 116.17, 110.69, 33.51, 17.09, 10.99. $C_{11}H_{11}N_3O_2$, EI-MS: m/z (M-H$^+$): 216.2 (calculated), 216.2 (found).

1-tert-butyl-6-cyclopropyl-3-methyl-1H-pyrazolo[3,4-b]pyridine-4-carboxylic acid (4j).—Yield: 21%. ^{1}H NMR (400 MHz, DMSO-d_6) δ 13.67 (s, 1H), 7.46 (s, 1H), 2.53 (s, 3H), 2.40 – 2.21 (m, 1H), 1.70 (s, 9H), 1.13 – 0.94 (m, 4H). ^{13}C NMR (101 MHz, DMSO-d_6) δ 166.96, 161.25, 151.40, 137.42, 133.83, 114.86, 109.86, 58.78, 28.65, 16.68, 15.45, 11.01. $C_{15}H_{19}N_3O_2$, EI-MS: m/z (M-H$^+$): 272.3 (calculated), 272.3 (found).

1-tert-butyl-3,6-dimethyl-1H-pyrazolo[3,4-b]pyridine-4-carboxylic acid (4k).—
Yield: 18%. ^{1}H NMR (400 MHz, DMSO-d_6) δ 7.34 (s, 1H), 2.62 (s, 3H), 2.53 (s, 3H), 1.73 (s, 9H). ^{13}C NMR (101 MHz, DMSO-d_6) δ 166.97, 156.46, 151.29, 137.34, 134.29, 115.96,

109.75, 59.00, 28.74, 24.52, 15.44. $C_{13}H_{17}N_3O_2$, EI-MS: m/z (M-H$^+$): 246.3 (calculated), 246.3 (found).

6-cyclopropyl-1-propyl-1H-pyrazolo[3,4-b]pyridine-4-carboxylic acid (4l).—
Yield: 35%. ^{1}H NMR (400 MHz, DMSO-d_6) δ 13.76 (brs, 1H), 8.22 (s, 1H), 7.59 (s, 1H), 4.35 (t, J = 6.8 Hz, 2H), 2.44 – 2.30 (m, 1H), 1.95 – 1.76 (m, 2H), 1.18 – 0.98 (m, 4H), 0.78 (t, J = 7.4 Hz, 3H). ^{13}C NMR (101 MHz, DMSO-d_6) δ 166.16, 163.06, 150.98, 131.74, 131.58, 116.23, 110.68, 47.85, 22.42, 17.03, 11.06. $C_{13}H_{15}N_3O_2$, EI-MS: m/z (M-H$^+$): 244.3 (calculated), 244.3 (found).

1-(butan-2-yl)-6-cyclopropyl-1H-pyrazolo[3,4-b]pyridine-4-carboxylic acid (4m).
—Yield: 38%. ^{1}H NMR (400 MHz, DMSO-d_6) δ 8.24 (s, 1H), 7.60 (s, 1H), 4.97 – 4.79 (m, 1H), 2.44 – 2.30 (m, 1H), 2.03 – 1.75 (m, 2H), 1.47 (d, J = 6.7 Hz, 3H), 1.18 – 0.98 (m, 4H), 0.62 (t, J = 7.3 Hz, 3H). ^{13}C NMR (101 MHz, DMSO-d_6) δ 166.22, 162.79, 150.90, 131.74, 116.21, 110.79, 53.73, 28.79, 20.04, 17.01, 11.07, 11.05, 10.62. $C_{14}H_{17}N_3O_2$, EI-MS: m/z (M-H$^+$): 258.3 (calculated), 258.3 (found).

6-cyclopropyl-1-(1-cyclopropylethyl)-1H-pyrazolo[3,4-b]pyridine-4-carboxylic acid (4n).—Yield: 29%. ^{1}H NMR (400 MHz, DMSO-d_6) δ 8.25 (s, 1H), 7.58 (s, 1H), 4.34 – 4.15 (m, 1H), 2.44 – 2.27 (m, 1H), 1.61 (d, J = 6.8 Hz, 3H), 1.46 – 1.28 (m, 1H), 1.14 – 0.95 (m, 4H), 0.65 – 0.49 (m, 1H), 0.47 – 0.37 (m, 1H), 0.37 – 0.13 (m, 2H). ^{13}C NMR (101 MHz, DMSO-d_6) δ 166.36, 162.63, 150.51, 131.72, 116.19, 111.16, 57.16, 19.63, 17.23, 16.98, 10.96, 10.91, 3.70, 3.55. $C_{15}H_{17}N_3O_2$, EI-MS: m/z (M-H$^+$): 270.3 (calculated), 270.3 (found).

6-cyclopropyl-N-(2-methoxyethyl)-1-(propan-2-yl)-1H-pyrazolo[3,4-b]pyridine-4-carboxamide (7a).—Yield: 75%. ^{1}H NMR (400 MHz, DMSO-d_6) δ 8.80 (s, 1H), 8.20 (d, J = 0.5 Hz, 1H), 7.42 (s, 1H), 5.21 – 5.00 (m, 1H), 3.57 – 3.42 (m, 4H), 3.29 (s, 3H), 2.34 – 2.16 (m, 1H), 1.47 (d, J = 6.7 Hz, 6H), 1.13 – 1.02 (m, 4H). ^{13}C NMR (101 MHz, DMSO-d_6) δ 166.45, 164.90, 149.58, 136.33, 131.55, 112.73, 110.96, 59.50, 47.93, 42.08, 36.08, 22.36, 21.81. $C_{16}H_{22}N_4O_2$, EI-MS: m/z (M+H$^+$): 303.4 (calculated), 303.4 (found). HPLC purity: 100%.

6-cyclopropyl-1-(propan-2-yl)-N-[2-(pyrrolidin-1-yl)ethyl]-1H-pyrazolo[3,4-b]pyridine-4-carboxamide (7b).—Yield: 72%. ^{1}H NMR (400 MHz, DMSO-d_6) δ 9.02 (t, J = 5.7 Hz, 1H), 8.24 (s, 1H), 7.56 (s, 1H), 5.21 – 5.00 (m, 1H), 3.67 – 3.48 (m, 2H), 3.14 – 2.79 (m, 6H), 2.32 – 2.21 (m, 1H), 1.91 – 1.71 (m, 4H), 1.46 (d, J = 6.7 Hz, 7H), 1.17 – 1.03 (m, 4H). ^{13}C NMR (101 MHz, DMSO-d_6) δ 164.90, 162.64, 149.83, 135.37, 131.58, 113.08, 110.70, 53.66, 53.24, 47.89, 36.89, 22.79, 21.74, 17.44, 10.78. $C_{19}H_{27}N_5O$, EI-MS: m/z (M+H$^+$): 342.5 (calculated), 342.5 (found). HPLC purity: 97.8%.

6-cyclopropyl-N-[2-(diethylamino)ethyl]-1-(propan-2-yl)-1H-pyrazolo[3,4-b]pyridine-4-carboxamide (7c).—Yield: 81%. ^{1}H NMR (400 MHz, DMSO-d_6) δ 8.69 (s, 1H), 8.22 (s, 1H), 7.40 (s, 1H), 5.20 – 5.04 (m, 1H), 3.51 – 3.31 (m, 2H), 2.71 – 2.61 (m, 2H), 2.61 – 2.52 (m, 4H), 2.33 – 2.20 (m, 1H), 1.47 (d, J = 6.7 Hz, 6H), 1.14 – 1.03 (m, 4H), 0.99 (t, J = 7.1 Hz, 6H). ^{13}C NMR (101 MHz, DMSO-d_6) δ 164.66, 162.56, 149.82,

135.89, 131.49, 112.87, 110.67, 51.10, 47.89, 46.63, 37.22, 21.72, 17.35, 11.58, 10.76. $C_{19}H_{29}N_5O$, EI-MS: m/z (M+H$^+$): 344.5 (calculated), 344.5 (found). HPLC purity: 98.0%.

6-cyclopropyl-N-[2-(dimethylamino)ethyl]-1-(propan-2-yl)-1H-pyrazolo[3,4-b]pyridine-4-carboxamide (7d).—Yield: 79%. ^{1}H NMR (400 MHz, DMSO-d_6) δ 8.73 (t, J = 5.7 Hz, 1H), 8.22 (s, 1H), 7.44 (s, 1H), 5.23 – 5.02 (m, 1H), 3.53 – 3.37 (m, 2H), 2.56 (t, J = 6.7 Hz, 2H), 2.28 (s, 7H), 1.47 (d, J = 6.7 Hz, 6H), 1.08 (d, J = 6.4 Hz, 4H). ^{13}C NMR (101 MHz, DMSO-d_6) δ 164.71, 162.56, 149.83, 135.77, 131.53, 112.97, 110.71, 57.60, 47.88, 44.78, 36.92, 21.73, 17.35, 10.75. $C_{17}H_{25}N_5O$, EI-MS: m/z (M+H$^+$): 316.4 (calculated), 316.4 (found). HPLC purity: 96.9%.

N-(azetidin-3-yl)-6-cyclopropyl-1-(propan-2-yl)-1H-pyrazolo[3,4-b]pyridine-4-carboxamide (7e).—TFA salt. Yield: 65%. ^{1}H NMR (400 MHz, DMSO-d_6) δ 9.57 (d, J = 6.7 Hz, 1H), 9.16 (s, 2H), 8.25 (s, 1H), 7.52 (s, 1H), 5.24 – 5.03 (m, 1H), 4.99 – 4.79 (m, 1H), 4.35 – 4.05 (m, 4H), 2.37 – 2.19 (m, 1H), 1.48 (d, J = 6.7 Hz, 6H), 1.18 – 1.04 (m, 4H). ^{13}C NMR (101 MHz, DMSO-d_6) δ 164.79, 162.71, 149.88, 134.65, 131.52, 113.24, 110.56, 51.83, 48.02, 41.52, 21.76, 17.40, 10.85. $C_{16}H_{21}N_5O$, EI-MS: m/z (M+H$^+$): 300.4 (calculated), 300.4 (found). HPLC purity: 98.6%.

6-cyclopropyl-N-[1-(dimethylamino)propan-2-yl]-1-(propan-2-yl)-1H-pyrazolo[3,4-b]pyridine-4-carboxamide (7f).—Yield: 86%. ^{1}H NMR (400 MHz, DMSO-d_6) δ 8.52 (d, J = 8.2 Hz, 1H), 8.22 (s, 1H), 7.46 (s, 1H), 5.24 – 5.03 (m, 1H), 4.34 – 4.16 (m, 1H), 2.63 – 2.50 (m, 1H), 2.42 – 2.18 (m, 8H), 1.48 (d, J = 6.7 Hz, 6H), 1.19 (d, J = 6.6 Hz, 3H), 1.15 – 1.04 (m, 4H). ^{13}C NMR (101 MHz, DMSO-d_6) δ 164.18, 162.48, 149.81, 136.13, 131.60, 113.13, 110.79, 63.65, 47.86, 45.03, 42.83, 21.74, 21.71, 18.73, 17.30, 10.73, 10.71. $C_{18}H_{27}N_5O$, EI-MS: m/z (M+H$^+$): 330.4 (calculated), 330.4 (found). HPLC purity: 98.4%.

6-cyclopropyl-N-(1-methylpyrrolidin-3-yl)-1-(propan-2-yl)-1H-pyrazolo[3,4-b]pyridine-4-carboxamide (7g).—Yield: 77%. ^{1}H NMR (400 MHz, CDCl$_3$) δ 8.27 (s, 1H), 7.97 (d, J = 8.4 Hz, 1H), 7.42 (s, 1H), 5.27 – 5.13 (m, 1H), 5.04 – 4.84 (m, 1H), 3.56 – 3.40 (m, 1H), 3.38 – 3.22 (m, 1H), 2.96 – 2.83 (m, 1H), 2.67 (s, 3H), 2.65 – 2.48 (m, 2H), 2.27 – 2.15 (m, 1H), 2.15 – 2.02 (m, 1H), 1.55 (d, J = 6.7 Hz, 6H), 1.22 – 1.13 (m, 2H), 1.10 – 0.99 (m, 2H). ^{13}C NMR (101 MHz, CDCl$_3$) δ 165.43, 163.48, 150.69, 134.62, 131.61, 113.55, 111.00, 62.30, 54.87, 49.01, 48.64, 41.15, 32.51, 22.08, 17.94, 11.19. $C_{18}H_{25}N_5O$, EI-MS: m/z (M+H$^+$): 328.4 (calculated), 328.4 (found). HPLC purity: 95.6%.

6-cyclopropyl-N-[2-(methylamino)ethyl]-1-(propan-2-yl)-1H-pyrazolo[3,4-b]pyridine-4-carboxamide (7h).—TFA salt. Yield: 72%. ^{1}H NMR (400 MHz, DMSO-d_6) δ 9.04 (t, J = 5.7 Hz, 1H), 8.77 (s, 2H), 8.25 (s, 1H), 7.49 (s, 1H), 5.23 – 5.01 (m, 1H), 3.63 (q, J = 5.9 Hz, 2H), 3.23 – 3.07 (m, 2H), 2.62 (s, 3H), 2.35 – 2.18 (m, 1H), 1.47 (d, J = 6.7 Hz, 6H), 1.16 – 1.01 (m, 4H). ^{13}C NMR (101 MHz, DMSO-d_6) δ 165.51, 162.60, 149.90, 135.20, 131.68, 113.25, 110.69, 47.97, 47.66, 35.69, 32.59, 21.76, 17.40, 10.77. $C_{16}H_{23}N_5O$, EI-MS: m/z (M+H$^+$): 302.4 (calculated), 302.4 (found). HPLC purity: 96.9%.

N-(2-aminoethyl)-6-cyclopropyl-1-(propan-2-yl)-1H-pyrazolo[3,4-b]pyridine-4-carboxamide (7i).—TFA salt. Yield: 68%. ^{1}H NMR (400 MHz, CD$_3$OD) δ 8.26 (s, 1H), 7.46 (s, 1H), 5.28 – 5.10 (m, 1H), 3.77 (t, J = 5.9 Hz, 2H), 3.28 (t, J = 5.9 Hz, 2H), 2.31 – 2.18 (m, 1H), 1.51 (d, J = 6.8 Hz, 6H), 1.22 – 1.00 (m, 4H). ^{13}C NMR (101 MHz, CD$_3$OD) δ 168.93, 165.18, 151.68, 136.17, 133.00, 132.91, 114.94, 112.00, 49.84, 40.66, 38.69, 22.13, 18.42, 11.57. C$_{15}$H$_{21}$N$_5$O, EI-MS: m/z (M+H$^+$): 288.4 (calculated), 288.4 (found). HPLC purity: 97.6%.

N-(1-aminopropan-2-yl)-6-cyclopropyl-1-(propan-2-yl)-1H-pyrazolo[3,4-b]pyridine-4-carboxamide (7j).—TFA salt. Yield: 81%. ^{1}H NMR (400 MHz, DMSO-d_6) δ 8.82 (d, J = 8.1 Hz, 1H), 8.24 (s, 1H), 8.13 (s, 3H), 7.56 (s, 1H), 5.21 – 5.04 (m, 1H), 4.45 – 4.24 (m, 1H), 3.12 – 2.93 (m, 2H), 2.35 – 2.22 (m, 1H), 1.48 (dd, J = 6.7, 1.2 Hz, 6H), 1.26 (d, J = 6.7 Hz, 3H), 1.18 – 1.04 (m, 4H). ^{13}C NMR (101 MHz, DMSO-d_6) δ 164.98, 162.54, 149.91, 135.54, 131.75, 113.47, 110.83, 47.96, 43.57, 43.06, 21.78, 21.76, 17.96, 17.38, 10.78, 10.68. C$_{16}$H$_{23}$N$_5$O, EI-MS: m/z (M+H$^+$): 302.4 (calculated), 302.4 (found). HPLC purity: 100.0%.

6-cyclopropyl-N-[3-(diethylamino)propyl]-1-(propan-2-yl)-1H-pyrazolo[3,4-b]pyridine-4-carboxamide (7k).—Yield: 86%. ^{1}H NMR (400 MHz, CD$_3$OD) δ 8.24 (s, 1H), 7.46 (s, 1H), 5.34 – 5.11 (m, 1H), 3.58 (t, J = 6.6 Hz, 2H), 3.30 – 3.13 (m, 6H), 2.38 – 2.23 (m, 1H), 2.20 – 1.98 (m, 2H), 1.55 (d, J = 6.8 Hz, 6H), 1.35 (t, J = 7.3 Hz, 6H), 1.25 – 1.02 (m, 4H). ^{13}C NMR (101 MHz, CD$_3$OD) δ 168.59, 165.26, 151.77, 136.56, 132.85, 132.77, 114.83, 112.06, 50.85, 49.92, 48.43, 37.97, 25.43, 22.15, 18.46, 11.61, 9.27. C$_{20}$H$_{31}$N$_5$O, EI-MS: m/z (M+H$^+$): 358.5 (calculated), 358.5 (found). HPLC purity: 97.8%.

6-cyclopropyl-N-[3-(dimethylamino)propyl]-1-(propan-2-yl)-1H-pyrazolo[3,4-b]pyridine-4-carboxamide (7l).—Yield: 79%. ^{1}H NMR (400 MHz, DMSO-d_6) δ 8.78 (t, J = 5.6 Hz, 1H), 8.19 (s, 1H), 7.39 (s, 1H), 5.12 (hept, J = 6.7 Hz, 1H), 3.46 – 3.20 (m, 2H), 2.36 – 2.22 (m, 3H), 2.16 (s, 6H), 1.78 – 1.63 (m, 2H), 1.47 (d, J = 6.7 Hz, 6H), 1.15 – 1.01 (m, 4H). ^{13}C NMR (101 MHz, DMSO-d_6) δ 164.68, 162.56, 149.84, 135.85, 131.53, 112.92, 110.71, 56.31, 47.88, 44.46, 37.39, 26.27, 21.73, 17.37, 10.76. C$_{18}$H$_{27}$N$_5$O, EI-MS: m/z (M+H$^+$): 330.4 (calculated), 330.4 (found). HPLC purity: 97.4%.

6-cyclopropyl-N-[3-(methylamino)propyl]-1-(propan-2-yl)-1H-pyrazolo[3,4-b]pyridine-4-carboxamide (7m).—TFA salt. Yield: 65%. ^{1}H NMR (400 MHz, DMSO-d_6) δ 8.98 (t, J = 5.7 Hz, 1H), 8.79 (s, 2H), 8.22 (s, 1H), 7.46 (s, 1H), 5.21 – 5.03 (m, 1H), 3.40 (q, J = 6.4 Hz, 2H), 3.05 – 2.89 (m, 2H), 2.65 – 2.54 (m, 3H), 2.40 – 2.21 (m, 1H), 1.90 (p, J = 6.9 Hz, 2H), 1.46 (d, J = 6.7 Hz, 6H), 1.08 (d, J = 6.4 Hz, 4H). ^{13}C NMR (101 MHz, DMSO-d_6) δ 165.13, 162.66, 149.91, 135.59, 131.60, 113.07, 110.73, 47.97, 46.18, 36.32, 32.41, 25.70, 21.76, 17.38, 10.80. C$_{17}$H$_{25}$N$_5$O, EI-MS: m/z (M+H$^+$): 316.4 (calculated), 316.4 (found). HPLC purity: 98.3%.

N-[2-(dimethylamino)ethyl]-1,6-bis(propan-2-yl)-1H-pyrazolo[3,4-b]pyridine-4-carboxamide (10a).—Yield: 84%. ^{1}H NMR (400 MHz, DMSO-d_6) δ 8.72 (t, J = 5.7 Hz, 1H), 8.28 (s, 1H), 7.50 (s, 1H), 5.31 – 5.13 (m, 1H), 3.53 – 3.39 (m, 2H), 3.27 – 3.13 (m, 1H), 2.56 – 2.49 (m, 2H), 2.25 (s, 6H), 1.51 (d, J

= 6.7 Hz, 6H), 1.35 (d, J = 6.9 Hz, 6H). ^{13}C NMR (101 MHz, DMSO-d_6) δ 166.44, 164.69, 149.57, 136.29, 131.48, 112.69, 110.93, 57.81, 47.92, 45.00, 37.14, 36.04, 22.35, 21.79. $C_{17}H_{27}N_5O$, EI-MS: m/z (M+H$^+$): 318.4 (calculated), 318.4 (found). HPLC purity: 96.3%.

N-(2-hydroxyethyl)-1,6-bis(propan-2-yl)-1H-pyrazolo[3,4-b]pyridine-4-carboxamide (10b).—Yield: 73%. ^{1}H NMR (400 MHz, DMSO-d_6) δ 8.74 (t, J = 5.6 Hz, 1H), 8.26 (d, J = 0.5 Hz, 1H), 7.51 (s, 1H), 5.30 – 5.08 (m, 1H), 4.79 (t, J = 5.6 Hz, 1H), 3.57 (q, J = 5.9 Hz, 2H), 3.40 (q, J = 6.0 Hz, 2H), 3.19 (h, J = 6.9 Hz, 1H), 1.50 (d, J = 6.7 Hz, 6H), 1.34 (d, J = 6.9 Hz, 6H). ^{13}C NMR (101 MHz, DMSO-d_6) δ 166.45, 164.90, 149.58, 136.33, 131.55, 112.73, 110.96, 59.50, 47.93, 42.08, 36.08, 22.36, 21.81. $C_{15}H_{22}N_4O_2$, EI-MS: m/z (M+H$^+$): 291.4 (calculated), 291.4 (found). HPLC purity: 100.0%.

N-[1-(dimethylamino)propan-2-yl]-1,6-bis(propan-2-yl)-1H-pyrazolo[3,4-b]pyridine-4-carboxamide (10c).—Yield: 75%. ^{1}H NMR (400 MHz, CD$_3$OD) δ 8.29 (s, 1H), 7.51 (s, 1H), 5.43 – 5.24 (m, 1H), 4.53 – 4.32 (m, 1H), 3.31 – 3.19 (m, 1H), 2.83 – 2.65 (m, 1H), 2.51 – 2.29 (m, 7H), 1.59 (d, J = 6.7, 1.5 Hz, 6H), 1.42 (d, J = 6.9, 1.5 Hz, 6H), 1.31 (d, J = 6.6, 1.5 Hz, 3H). ^{13}C NMR (101 MHz, CD$_3$OD) δ 168.93, 167.84, 151.45, 137.96, 132.96, 114.36, 112.48, 65.31, 49.90, 45.74, 44.78, 38.04, 22.91, 22.89, 22.23, 19.34. $C_{18}H_{29}N_5O$, EI-MS: m/z (M+H$^+$): 332.5 (calculated), 332.4 (found). HPLC purity: 98.8%.

N-[2-(methylamino)ethyl]-1,6-bis(propan-2-yl)-1H-pyrazolo[3,4-b]pyridine-4-carboxamide (10d).—TFA salt. Yield: 71%. ^{1}H NMR (400 MHz, DMSO-d_6) δ 9.18 (t, J = 5.6 Hz, 1H), 9.00 (s, 2H), 8.30 (s, 1H), 7.61 (s, 1H), 5.32 – 5.08 (m, 1H), 3.65 (q, J = 5.9 Hz, 2H), 3.28 – 3.09 (m, 3H), 2.62 (s, 3H), 1.49 (d, J = 6.7 Hz, 6H), 1.33 (d, J = 6.9 Hz, 6H). ^{13}C NMR (101 MHz, DMSO-d_6) δ 166.55, 165.52, 149.68, 135.63, 131.69, 113.11, 110.97, 48.02, 47.62, 36.14, 35.72, 32.52, 22.35, 21.83. $C_{16}H_{25}N_5O$, EI-MS: m/z (M+H$^+$): 304.4 (calculated), 304.4 (found). HPLC purity: 97.5%.

N-(2-aminoethyl)-1,6-bis(propan-2-yl)-1H-pyrazolo[3,4-b]pyridine-4-carboxamide (10e).—TFA salt. Yield: 80%. ^{1}H NMR (400 MHz, DMSO-d_6) δ 9.09 (t, J = 5.6 Hz, 1H), 8.29 (s, 1H), 8.12 (brs, 3H), 7.59 (s, 1H), 5.35 – 5.09 (m, 1H), 3.59 (q, J = 6.0 Hz, 2H), 3.29 – 3.12 (m, 1H), 3.13 – 2.96 (m, 2H), 1.50 (d, J = 6.7 Hz, 6H), 1.34 (d, J = 6.9 Hz, 6H). ^{13}C NMR (101 MHz, DMSO-d_6) δ 166.53, 165.49, 149.64, 135.72, 131.65, 113.06, 110.93, 48.00, 38.34, 37.10, 36.13, 22.36, 21.84. $C_{15}H_{23}N_5O$, EI-MS: m/z (M+H$^+$): 290.4 (calculated), 290.4 (found). HPLC purity: 97.2%.

N-(1-aminopropan-2-yl)-1,6-bis(propan-2-yl)-1H-pyrazolo[3,4-b]pyridine-4-carboxamide (10f).—TFA salt. Yield: 73%. ^{1}H NMR (400 MHz, DMSO-d_6) δ 8.78 (d, J = 8.1 Hz, 1H), 8.27 (s, 1H), 8.04 (brs, 3H), 7.57 (s, 1H), 5.31 – 5.10 (m, 1H), 4.46 – 4.20 (m, 1H), 3.29 – 3.13 (m, 1H), 3.11 – 2.94 (m, 2H), 1.50 (d, J = 6.7, 1.3 Hz, 6H), 1.34 (d, J = 6.9 Hz, 6H), 1.26 (d, J = 6.8 Hz, 3H). ^{13}C NMR (101 MHz, DMSO-d_6) δ 166.41, 165.00, 149.63, 135.99, 131.68, 113.10, 111.02, 47.98, 43.56, 43.09, 36.09, 22.36, 21.82, 21.79, 17.94. $C_{16}H_{25}N_5O$, EI-MS: m/z (M+H$^+$): 304.4 (calculated), 304.4 (found). HPLC purity: 99.0%.

6-tert-butyl-N-[2-(dimethylamino)ethyl]-1-(propan-2-yl)-1H-pyrazolo[3,4-b]pyridine-4-carboxamide (11a).—Yield: 83%. ^{1}H NMR (400

MHz, CD$_3$OD) δ 8.27 (s, 1H), 7.68 (s, 1H), 5.38

– 5.20 (m, 1H), 3.72 – 3.56 (m, 2H), 2.79 (t, J = 6.6 Hz, 2H), 2.47 (s, 6H), 1.62

– 1.51 (m, 6H), 1.46 (d, J = 1.4 Hz, 9H). ^{13}C NMR (101 MHz, CD$_3$OD) δ 168.93, 165.18, 151.68, 136.17, 133.00, 132.91, 114.94, 112.00, 49.84, 40.66, 38.69, 22.13, 18.42, 11.57. C$_{18}$H$_{29}$N$_5$O, EI-MS: m/z (M+H$^+$): 332.5 (calculated), 332.4 (found). HPLC purity: 97.9%.

N-(2-aminoethyl)-6-tert-butyl-1-(propan-2-yl)-1H-pyrazolo[3,4-b]pyridine-4-carboxamide (11b).—TFA salt. Yield: 78%. ^{1}H NMR (400 MHz,

DMSO-d_6) δ 9.11 (t, J = 5.6 Hz, 1H), 8.29 (s, 1H), 8.06

(brs, 3H), 7.74 (s, 1H), 5.30 – 5.09 (m, 1H), 3.60 (q, J = 6.1 Hz, 2H), 3.14 – 2.98

(m, 2H), 1.51 (d, J = 6.7 Hz, 6H), 1.43 (s, 9H). ^{13}C NMR (101 MHz, DMSO-d_6) δ 168.43, 165.62, 149.20, 135.52, 131.50, 111.43, 110.56, 48.33, 38.37, 37.97, 37.09, 29.99, 21.74. C$_{16}$H$_{25}$N$_5$O, EI-MS: m/z (M+H$^+$): 304.4 (calculated), 304.4 (found). HPLC purity: 96.8%.

N-[2-(dimethylamino)ethyl]-6-methyl-1-(propan-2-yl)-1H-pyrazolo[3,4-b]pyridine-4-carboxamide (12a).—Yield: 77%. ^{1}H NMR (400

MHz, DMSO-d_6) δ 8.73 (t, J = 5.7 Hz, 1H), 8.26

(s, 1H), 7.47 (s, 1H), 5.30 – 5.08 (m, 1H), 3.52 – 3.36 (m, 2H), 2.66 (s, 3H), 2.58 (t, J = 6.6 Hz, 2H), 2.30 (s, 6H), 1.48 (d, J = 6.7 Hz, 6H). ^{13}C NMR (101 MHz, DMSO-d_6) δ 164.68, 157.80, 149.71, 135.97, 131.57, 114.96, 110.45, 57.49, 47.61, 44.67, 36.81, 24.49, 21.89. C$_{15}$H$_{23}$N$_5$O, EI-MS: m/z (M+H$^+$): 290.4 (calculated), 290.4 (found). HPLC purity: 99.1%.

6-methyl-N-(1-methylpyrrolidin-3-yl)-1-(propan-2-yl)-1H-pyrazolo[3,4-b]pyridine-4-carboxamide (12b).—Yield: 65%. ^{1}H NMR (400

MHz, DMSO-d_6) δ 8.94 (d, J = 7.0 Hz, 1H), 8.24 (s, 1H), 7.55

(s, 1H), 5.30 – 5.08 (m, 1H), 4.59 – 4.41 (m, 1H), 3.02 – 2.92 (m, 1H), 2.92 – 2.78 (m, 1H), 2.78 – 2.69 (m, 1H), 2.69 – 2.59 (m, 4H), 2.42 (s, 3H), 2.34 – 2.16 (m, 1H), 2.00 – 1.82 (m, 1H), 1.48 (d, J = 6.7 Hz, 6H). ^{13}C NMR (101 MHz, DMSO-d_6) δ 164.54, 157.76, 149.70, 135.67, 131.61, 115.14, 110.53, 61.04, 54.40, 48.95, 47.60, 41.19, 31.05, 24.46, 21.89. C$_{16}$H$_{23}$N$_5$O, EI-MS: m/z (M+H$^+$): 302.4 (calculated), 302.4 (found). HPLC purity: 100.0%.

6-methyl-N-(1-methylazetidin-3-yl)-1-(propan-2-yl)-1H-pyrazolo[3,4-b]pyridine-4-carboxamide (12c).—Yield: 65%. ^{1}H NMR

(400 MHz, DMSO-d_6) δ 9.20 (d, J = 7.0 Hz, 1H), 8.24 (s, 1H), 7.53 (s, 1H),

5.33 – 5.13 (m, 1H), 4.62 – 4.42 (m, 1H), 3.77 – 3.60 (m, 2H), 3.23 – 3.12 (m, 2H), 2.67 (s, 3H), 2.34 (s, 3H), 1.48 (d, J = 6.7 Hz, 6H). ^{13}C NMR (101 MHz, DMSO-d_6) δ 164.31, 157.79, 149.71, 135.41, 131.58, 115.05, 110.45, 62.15, 47.62, 45.04, 39.81, 24.48, 21.89. C$_{15}$H$_{21}$N$_5$O, EI-MS: m/z (M+H$^+$): 288.4 (calculated), 288.3 (found). HPLC purity: 98.5%.

6-methyl-N-[2-(methylamino)ethyl]-1-(propan-2-yl)-1H-pyrazolo[3,4-b]pyridine-4-carboxamide (12d).—TFA salt. Yield: 74%.

^{1}H NMR (400 MHz, DMSO-d_6) δ 9.04 (t, J = 5.6 Hz, 1H), 8.86 (brs, 2H), 8.29

(s, 1H), 7.52 (s, 1H), 5.33 – 5.07 (m, 1H), 3.72 – 3.55 (m, 2H), 3.22 – 3.09 (m, 2H), 2.66

(s, 3H), 2.62 (s, 3H), 1.48 (d, J = 6.7 Hz, 6H). ^{13}C NMR (101 MHz, DMSO-d_6) δ 165.44,

157.79, 149.79, 135.44, 131.73, 115.21, 110.46, 47.69, 47.61, 35.70, 32.54, 24.48, 21.91. $C_{14}H_{21}N_5O$, EI-MS: m/z (M+H$^+$): 276.4 (calculated), 276.3 (found). HPLC purity: 97.6%.

N-(2-aminoethyl)-6-methyl-1-(propan-2-yl)-1H-pyrazolo[3,4-b]pyridine-4-carboxamide (12e).—TFA salt. Yield: 65%. ^{1}H NMR (400 MHz, DMSO-d_6) δ 9.00 (t, J = 5.6 Hz, 1H), 8.29 (s, 1H), 8.09 (s, 3H), 7.52 (s, 1H), 5.29 – 5.09 (m, 1H), 3.64 – 3.53 (m, 2H), 3.13 – 2.98 (m, 2H), 2.66 (s, 3H), 1.48 (d, J = 6.7 Hz, 6H). ^{13}C NMR (101 MHz, DMSO-d_6) δ 165.41, 157.81, 149.79, 135.54, 131.72, 115.22, 110.46, 47.70, 38.34, 37.10, 24.49, 21.92. $C_{13}H_{19}N_5O$, EI-MS: m/z (M+H$^+$): 262.3 (calculated), 262.3 (found). HPLC purity: 98.5%.

1-cyclopentyl-N-[2-(dimethylamino)ethyl]-6-methyl-1H-pyrazolo[3,4-b]pyridine-4-carboxamide (13).—Yield: 69%. ^{1}H NMR (400 MHz, DMSO-d_6) δ 8.75 (t, J = 5.6 Hz, 1H), 8.26 (s, 1H), 7.47 (s, 1H), 5.48 – 5.25 (m, 1H), 3.53 – 3.38 (m, 2H), 2.66 (s, 3H), 2.62 (t, J = 6.6 Hz, 2H), 2.32 (s, 6H), 2.16 – 2.04 (m, 2H), 2.04 – 1.81 (m, 4H), 1.80 – 1.59 (m, 2H). ^{13}C NMR (101 MHz, DMSO-d_6) δ 164.71, 157.85, 150.28, 135.93, 131.67, 115.00, 110.49, 57.41, 56.45, 44.55, 36.71, 31.97, 24.48, 24.22. $C_{17}H_{25}N_5O$, EI-MS: m/z (M+H$^+$): 316.4 (calculated), 316.4 (found). HPLC purity: 100.0%.

N-[2-(dimethylamino)ethyl]-6-methyl-1-propyl-1H-pyrazolo[3,4-b]pyridine-4-carboxamide (14).—Yield: 70%. ^{1}H NMR (400 MHz, DMSO-d_6) δ 8.73 (t, J = 5.7 Hz, 1H), 8.25 (s, 1H), 7.47 (s, 1H), 4.39 (t, J = 7.0 Hz, 2H), 3.53 – 3.35 (m, 2H), 2.65 (s, 3H), 2.56 (t, J = 6.7 Hz, 2H), 2.28 (s, 6H), 1.95 – 1.79 (m, 2H), 0.82 (t, J = 7.4 Hz, 3H). ^{13}C NMR (101 MHz, DMSO-d_6) δ 164.64, 158.06, 150.62, 135.98, 131.70, 114.91, 110.25, 57.57, 47.81, 44.74, 36.89, 24.49, 22.48, 11.01. $C_{15}H_{23}N_5O$, EI-MS: m/z (M+H$^+$): 290.4 (calculated), 290.4 (found). HPLC purity: 100.0%.

N-[2-(dimethylamino)ethyl]-1-ethyl-6-methyl-1H-pyrazolo[3,4-b]pyridine-4-carboxamide (15a).—Yield: 73%. ^{1}H NMR (400 MHz, DMSO-d_6) δ 8.80 (t, J = 5.7 Hz, 1H), 8.26 (s, 1H), 7.51 (s, 1H), 4.47 (q, J = 7.2 Hz, 2H), 3.52 – 3.39 (m, 2H), 2.66 (s, 3H), 2.61 (t, J = 6.6 Hz, 2H), 2.32 (s, 6H), 1.41 (t, J = 7.2 Hz, 3H). ^{13}C NMR (101 MHz, DMSO-d_6) δ 164.64, 158.06, 150.11, 135.93, 131.73, 114.97, 110.38, 57.42, 44.56, 41.27, 36.72, 24.47, 14.74. $C_{14}H_{21}N_5O$, EI-MS: m/z (M+H$^+$): 276.4 (calculated), 276.3 (found). HPLC purity: 98.9%.

1-ethyl-6-methyl-N-[2-(methylamino)ethyl]-1H-pyrazolo[3,4-b]pyridine-4-carboxamide (15b).—TFA salt. Yield: 63%. ^{1}H NMR (400 MHz, DMSO-d_6) δ 9.04 (t, J = 5.5 Hz, 1H), 8.29 (s, 1H), 8.14 (brs, 2H), 7.54 (s, 1H), 4.47 (q, J = 7.2 Hz, 2H), 3.59 (q, J = 6.0 Hz, 2H), 3.16 – 2.94 (m, 2H), 2.66 (s, 3H), 1.41 (t, J = 7.2 Hz, 3H). ^{13}C NMR (101 MHz, DMSO-d_6) δ 165.35, 158.06, 150.17, 135.54, 131.87, 115.19, 110.38, 41.34, 38.31, 37.11, 24.46, 14.77. $C_{13}H_{19}N_5O$, EI-MS: m/z (M+H$^+$): 262.3 (calculated), 262.3 (found). HPLC purity: 98.9%.

6-cyclopropyl-N-[2-(dimethylamino)ethyl]-1-ethyl-1H-pyrazolo[3,4-b]pyridine-4-carboxamide (16).—Yield: 86%. ^{1}H NMR (400 MHz, DMSO-d_6) δ 8.77 (t, J = 5.7 Hz, 1H), 8.22 (s, 1H), 7.46 (s, 1H), 4.42 (q, J = 7.2 Hz, 2H), 3.52 – 3.37 (m, 2H), 2.57

(t, J = 6.7 Hz, 2H), 2.35 – 2.21 (m, 7H), 1.39 (t, J = 7.2 Hz, 3H), 1.12 – 1.01 (m, 4H). ^{13}C NMR (101 MHz, DMSO-d_6) δ 164.66, 162.84, 150.19, 135.75, 131.73, 112.96, 110.55, 57.57, 44.73, 41.22, 36.89, 17.38, 14.61, 10.75. $C_{16}H_{23}N_5O$, EI-MS: m/z (M+H+): 302.4 (calculated), 302.4 (found). HPLC purity: 100%.

6-cyclopropyl-N-[2-(dimethylamino)ethyl]-1-methyl-1H-pyrazolo[3,4-b]pyridine-4-carboxamide (17).—Yield: 76%. ^{1}H NMR (400 MHz, DMSO-d_6) δ 8.73 (t, J = 5.7 Hz, 1H), 8.22 (s, 1H), 7.45 (s, 1H), 4.00 (s, 3H), 3.49 – 3.39 (m, 2H), 2.56 – 2.48 (m, 2H), 2.35 – 2.28 (m, 1H), 2.26 (s, 6H), 1.18 – 1.04 (m, 4H). ^{13}C NMR (101 MHz, DMSO-d_6) δ 164.60, 162.98, 150.74, 135.74, 131.70, 112.88, 110.42, 57.76, 44.97, 37.12, 33.41, 17.41, 10.70. $C_{15}H_{21}N_5O$, EI-MS: m/z (M+H+): 288.4 (calculated), 288.4 (found). HPLC purity: 98.2%.

1-tert-butyl-6-cyclopropyl-N-[2-(dimethylamino)ethyl]-3-methyl-1H-pyrazolo[3,4-b]pyridine-4-carboxamide (18a).—Yield: 69%. ^{1}H NMR (400 MHz, DMSO-d_6) δ 8.56 (t, J = 5.7 Hz, 1H), 7.07 (s, 1H), 3.45 – 3.29 (m, 2H), 2.46 (t, J = 6.7 Hz, 2H), 2.39 (s, 3H), 2.30 – 2.23 (m, 1H), 2.21 (s, 6H), 1.70 (s, 9H), 1.13 – 0.96 (m, 4H). ^{13}C NMR (101 MHz, DMSO-d_6) δ 166.10, 161.15, 150.94, 138.87, 137.32, 112.40, 109.80, 58.62, 57.71, 44.98, 37.01, 28.67, 16.81, 13.87, 10.80. $C_{19}H_{29}N_5O$, EI-MS: m/z (M+H+): 344.5 (calculated), 344.5 (found). HPLC purity: 98.3%.

1-tert-butyl-6-cyclopropyl-3-methyl-N-[2-(methylamino)ethyl]-1H-pyrazolo[3,4-b]pyridine-4-carboxamide (18b).—TFA salt. Yield: 53%. ^{1}H NMR (400 MHz, DMSO-d_6) δ 8.92– 8.81 (m, 3H), 7.23 (s, 1H), 3.60 (q, J = 6.1 Hz, 2H), 3.15 – 3.04 (m, 2H), 2.63 (s, 3H), 2.39 (s, 3H), 2.29 – 2.15 (m, 1H), 1.70 (s, 9H), 1.16 – 0.87 (m, 4H). ^{13}C NMR (101 MHz, DMSO-d_6) δ 166.66, 161.17, 151.06, 138.00, 137.46, 112.78, 109.78, 58.71, 48.53, 47.33, 35.49, 32.49, 28.70, 16.91, 14.36, 10.82. $C_{18}H_{27}N_5O$, EI-MS: m/z (M+H+): 330.4 (calculated), 330.4 (found). HPLC purity: 98.0%.

1-tert-butyl-N-[2-(dimethylamino)ethyl]-3,6-dimethyl-1H-pyrazolo[3,4-b]pyridine-4-carboxamide (19).—Yield: 83%. ^{1}H NMR (400 MHz, DMSO-d_6) δ 8.60 (t, J = 5.7 Hz, 1H), 7.02 (s, 1H), 3.49 – 3.37 (m, 3H), 2.60 (s, 3H), 2.54 (t, J = 6.7 Hz, 2H), 2.41 (s, 3H), 2.28 (s, 6H), 1.74 (s, 9H). ^{13}C NMR (101 MHz, DMSO-d_6) δ 166.11, 156.35, 150.88, 139.06, 137.27, 113.62, 109.67, 58.86, 57.46, 44.69, 36.72, 28.77, 24.64, 13.95. $C_{17}H_{27}N_5O$, EI-MS: m/z (M+H+): 318.4 (calculated), 318.4 (found). HPLC purity: 97.8%.

6-cyclopropyl-N-[2-(dimethylamino)ethyl]-1-propyl-1H-pyrazolo[3,4-b]pyridine-4-carboxamide (20).—Yield: 83%. ^{1}H NMR (400 MHz, DMSO-d_6) δ 8.79 (t, J = 5.7 Hz, 1H), 8.22 (s, 1H), 7.46 (s, 1H), 4.35 (t, J = 6.8 Hz, 2H), 3.47 (q, J = 6.4 Hz, 2H), 2.62 (t, J = 6.7 Hz, 2H), 2.33 (s, 6H), 2.31 – 2.20 (m, 1H), 1.92 – 1.78 (m, 2H), 1.17 – 1.01 (m, 4H), 0.79 (t, J = 7.4 Hz, 3H). ^{13}C NMR (101 MHz, DMSO-d_6) δ 164.74, 162.85, 150.75, 135.70, 131.75, 113.00, 110.38, 57.44, 47.73, 44.57, 36.72, 22.44, 17.37, 11.05, 10.79. $C_{17}H_{25}N_5O$, EI-MS: m/z (M+H+): 316.4 (calculated), 316.4 (found). HPLC purity: 98.9%.

1-(butan-2-yl)-6-cyclopropyl-N-[2-(dimethylamino)ethyl]-1H-pyrazolo[3,4-b]pyridine-4-carboxamide (21).—Yield: 78%. ^{1}H NMR (400 MHz, DMSO-d_6) δ 8.71 (t, J = 5.7 Hz, 1H), 8.24 (s, 1H), 7.43 (s, 1H), 5.00 – 4.79 (m, 1H), 3.45 (q, J = 6.4 Hz, 2H), 2.58 – 2.48 (m, 2H), 2.36 – 2.19 (m, 7H), 2.04 – 1.90 (m, 1H), 1.90 – 1.73 (m, 1H), 1.47 (d, J = 6.7 Hz, 3H), 1.21 – 0.95 (m, 4H), 0.63 (t, J = 7.3 Hz, 3H). ^{13}C NMR (101 MHz, DMSO-d_6) δ 164.72, 162.56, 150.66, 135.84, 131.69, 112.97, 110.47, 57.75, 53.54, 44.95, 37.09, 28.78, 20.07, 17.32, 10.80, 10.76, 10.62. $C_{18}H_{27}N_5O$, EI-MS: m/z (M+H^{+}): 330.4 (calculated), 330.4 (found). Purity: 98.2%.

6-cyclopropyl-1-(1-cyclopropylethyl)-N-[2-(dimethylamino)ethyl]-1H-pyrazolo[3,4-b]pyridine-4-carboxamide (22).—Yield: 71%. ^{1}H NMR (400 MHz, DMSO-d_6) δ 8.70 (t, J = 5.7 Hz, 1H), 8.23 (s, 1H), 7.43 (s, 1H), 4.41 – 4.18 (m, 1H), 3.50 – 3.37 (m, 2H), 2.58 – 2.47 (m, 2H), 2.34 – 2.19 (m, 7H), 1.62 (d, J = 6.8 Hz, 3H), 1.46 – 1.29 (m, 1H), 1.13 – 0.98 (m, 4H), 0.67 – 0.50 (m, 1H), 0.49 – 0.36 (m, 1H), 0.36 – 0.15 (m, 2H). ^{13}C NMR (101 MHz, DMSO-d_6) δ 164.71, 162.52, 150.24, 135.88, 131.49, 113.11, 110.61, 57.76, 57.03, 44.99, 37.13, 19.63, 17.27, 17.24, 10.79, 10.72, 3.65, 3.57. $C_{19}H_{27}N_5O$, EI-MS: m/z (M+H^{+}): 342.5 (calculated), 342.4 (found). HPLC purity: 97.4%.

1-(propan-2-yl)-N-(pyridin-2-yl)-6-(thiophen-2-yl)-1H-pyrazolo[3,4-b]pyridine-4-carboxamide (JX040).—Yield: 85%. ^{1}H NMR (400 MHz, DMSO-d_6) δ 11.30 (s, 1H), 8.47 (s, 1H), 8.46 – 8.42 (m, 1H), 8.36 (s, 1H), 8.29 (d, J = 1.0 Hz, 1H), 8.12 (dd, J = 3.8, 1.2 Hz, 1H), 7.96 – 7.85 (m, 1H), 7.75 (dd, J = 5.0, 1.1 Hz, 1H), 7.28 – 7.17 (m, 2H), 5.23 (hept, J = 6.6 Hz, 1H), 1.55 (d, J = 6.7 Hz, 6H). ^{13}C NMR (101 MHz, DMSO-d_6) δ 164.0, 151.7, 151.2, 149.7, 148.1, 144.0, 138.4, 135.9, 132.1, 129.8, 128.6, 128.0, 120.4, 115.0, 111.9, 111.6, 48.5, 21.9. HPLC purity: 100%.

Cell lines and Viruses

Rhabdomyosarcoma (RD, ATCC, CCL-136), A172 (ATCC, CRL-1620) and SH-SY5Y (ATCC, CRL-2266) were maintained in a 37 °C incubator in a 5% CO_2 atmosphere. RD cell was cultured in Dulbecco's modified Eagle's medium (DMEM) with 10% fetal bovine serum (FBS) and 1% penicillin-streptomycin (P/S). SH-SY5Y were cultured in 10% FBS and 1% P/S with 50% DMEM and 50% F-12 medium. All of the following EV-D68 strains used in this study were purchased from ATCC: US/KY/14-18953 (ATCC, NE-49132), US/MO/14-18947 (ATCC, NR-49129), US/MO/14-18949 (ATCC, NR-49130), US/IL/14-18952 (ATCC, NR-49131), US/IL/14-18956 (ATCC, NR-49133). All of the following EV-A71 strains used in this study were purchased from ATCC or BEI Resources: Tainan/4643/1998 (BEI Resources, NR-471), Enterovirus 71, MP4 (BEI Resources, NR-472). Enteroviruses A71 US/CT/2016- 19519 was obtained from Dr. William Nix at the Centers for Disease Control and Prevention under a material transfer agreement. All viruses were amplified in RD cells prior to infection assays.

CPE assays

CPE assays were carried out similarly as previously described.[33, 49] For EV-D68 CPE assays, RD cells were grown to over 90% confluency after seeding in the 96-well plate for 18-24 hrs, growth medium was aspirated and cells were washed with 200 μl PBS

buffer supplemented with magnesium and calcium. Cells were infected with EV-D68 viruses diluted in DMEM with 2% FBS and 30 mM $MgCl_2$ at a MOI of 0.01and incubated at 33 °C incubator in a 5% CO_2 atmosphere for 1-2 hrs. Testing compounds diluted in DMEM with 2% FBS and 30 mM $MgCl_2$ were added and cells were incubated in 33 °C incubator in a 5% CO_2 atmosphere for 3 days to develop complete CPE in virus infected cells. For EV-A71 CPE assays, similar procedures were performed on RD cells except that the 30 mM $MgCl_2$ was not included in the medium and infected cells were incubated at 37 °C instead of 33 °C, and the incubation time was typically 2.5 days for EV-A71 virus to develop complete CPE. For CVB3 virus CPE assay, Vero cells were used for infection with CVB3 Nancy virus at a MOI of 0.3 with similar procedure as EV-A71. For all CPE assays, growth media was aspirated and 50 μg/ml of neutral red staining solution was used to stain viable cells in each well. Absorbance at 540 nm was measured using a Multiskan FC Microplate Photometer (ThermoFisher Scientific). The EC_{50} values were calculated from best-fit dose response curves using GraphPad Prism 8.

Cytotoxicity assay

The cytotoxicity of each compound was determined using the neutral red cell viability assay. The assay was performed under similar conditions (incubation temperature, time, and media) as the CPE assay, but excluded viral infection. Data acquisition and analysis (CC_{50}) was performed similarly to the antiviral CPE assay, and all values are from triplicate experiments.

Plaque assay

Plaque assay for EV-D68 US/MO/14-18947 was performed as previously described.[38, 39] RD cells were grown to more than 90% confluent and washed with PBS supplemented with magnesium and calcium after removing the growth medium. Cells were infected by EV-D68 virus and incubated at 33 °C incubator for 1-2 hours to allow virus attachment. After washing the unbound viruses, an overlay containing the indicated concentration of test compounds and 1.2% Avicel (FMC BioPolymer, Philadelphia, PA) in DMEM supplemented with 2% FBS and 30 mM $MgCl_2$ was added with 4 ml per well. The plates were incubated at 33 °C (5% CO_2) incubator for 3 days and the cells were stained with crystal violet after removing the Avicel overlay. Plaque areas were quantified by ImageJ and plotted with drug concentration for the calculation of EC_{50} values.

Differential scanning fluorimetry (DSF)

The binding of compound **7d** to EV-A71 Tainan/4643/1998, EV-D68 US/MO/14-18947, and CVB3 Nancy 2C proteins was detected in DSF using a Thermal Fisher QuantStudio™ 5 RealTime PCR System as previously described.[46] 4 μM of EV-A71, EV-D68, and CVB WT 2C proteins were incubated with compound **7d** at 10, 30, 100 and 300 μM concentrations in a buffer containing 20 mM Hepes (pH7.5), 300 mM NaCl at 37 °C for 1 hr. For the EV-D68 2C-D183V, D323G and D183V/D323G mutant 2C proteins, **7d** was tested at 100 μM. 1 × SYPRO orange (Thermal Fisher) were added and the fluorescent signals were monitored under a temperature gradient ranging from 30 to 90 °C (incremental steps of 0.05 °C/s). As the temperature increases, test proteins gradually denatured and the melting

temperature (T_m) was calculated as the mid-log of the transition phase from the native to the denatured protein using a Boltzmann model in Protein Thermal Shift Software v1.3. T_m was calculated by subtracting reference melting temperature of proteins in the presence of DMSO from the T_m in the presence of indicated concentration of **7d**. Curve fittings were performed using the Boltzmann sigmoidal equation in Prism 8 software.

Immunofluorescence staining assay

Immunofluorescence staining was performed similarly as previously described,[38, 39, 45] with minor modifications. Neuronal cell line SH-SY5Y growing on cover slips (Nunc™ Thermanox™) were infected with EV-D68 US/MO/14-18947 at a MOI of 1. Virus were amplified in the presence of DMSO or indicated concentrations of testing compounds. At 18 hpi, cells were fixed with 4% formaldehyde for 10 min, followed by permeabilization with 0.2% Triton X-100 for another 10 min. After blocking with 3% bovine serum albumin (Sigma) at 4 °C overnight, cells were stained with rabbit anti-VP1 antibody at room temperature for 2 hrs and then with antirabbit immunoglobulin secondary antibody conjugated to Alexa Fluor 488. The nuclei were stained with 300 nM DAPI after secondary antibody incubation. Fluorescent images were acquired using a ZOE fluorescent Cell Imager (Bio-Rad).

Serial viral passage experiment and viral 2C gene sequencing

Serial viral passage experiments were carried out in the presence of compound **7d** by doubling the concentration from previous passage, starting with concentration of ~1xEC_{50} at P1. RD cells were infected with EV-D68 US/MO/14-18947 at a MOI of 0.1, and the amplified virus in the cell culture supernatant was collected after approximately 3 days when a significant cytopathic effect was observed, and viral titer was quantified by plaque assay. Drug sensitivity was tested in the P5 virus by determining the EC_{50} value through CPE assay. The viral genome RNA was purified using QIAGEN viral RNA mini kit, followed by reverse transcription using SuperScript III first strand reverse transcriptase (Invitrogen) with an oligo(dT) primer. The whole viral genome was sequenced via 14 sequencing reactions by Eton Biosciences, Inc. The sequencing primers were reported before.[39] Specifically, the fragment which contains whole 2C gene were PCR amplified using primers (Forward: 5'- GTTAGGTACACATATTGTTTGG-3' and Reverse: 5'- CTTTAGGTTTAG GATTGG GGATTCCTG-3'), and sequenced by Eton Bioscience, Inc using primer (5'- CAAGCCTTATTC AACAACGTCC-3' and 5'- CTTTAGGTTTAG GATTGG GGATTCCTG-3').

Generation of EV-D68 virus containing 2C mutants by reverse genetics

A plasmid-based reverse genetic system for EV-D68 US/MO/14-18947 was generated in pHH21 plasmid as previously described.[38, 39, 44] The 2C mutations were introduced via site-directed mutagenesis using Agilent Technologies QuikChange II XL kit according to the manufacturer's instructions and the inserted mutations were confirmed by sequencing. RD cells or HEK293T cells were transfected with the pHH21 plasmids containing US/MO/14-18947 genome (WT or 2C-D183V, D323G, D183V/D323G) using Lipofectamine 3000 Transfection Reagent (Thermo Fisher) according to the manufacture's instructions. The

generated virus in the cell culture medium were collected (3-5 days post transfection) and amplified on RD cells. The mutations in the viral 2C genes of the amplified viruses were confirmed by sequencing.

Virus growth competition assay

To compare the fitness of replication of WT virus (rWT) with the 2C mutant virus (r2C-D183V/D323G), virus growth competition assay was carried out. RD cells were infected by a virus mixture containing rWT and r2C-D183V/D323G at a ratio of 1:100 (MOI=0.1). The amplified virus from culture medium was collected 3 days post infection and viral titers were quantified by plaque assay and were used for the next round of infection. After 3 passages, viral 2C gene from each passage of the virus was sequenced as described in the serial passage experiment. The percentages of WT and 2C-D183V, D323G in each passage were estimated by measuring the height of the nucleotide peaks in the sequencing trace as previously described.[50]

Supplementary Material

Refer to Web version on PubMed Central for supplementary material.

ACKNOWLEDGEMENTS

ABBREVIATIONS USED

AFM	acute flaccid myelitis
CNS	central nervous system
CVB3	coxsackievirus B3
DSF	differential scanning fluorimetry
EV-A71	enterovirus A71
EV-D68	enterovirus D68

REFERENCES

1. Baggen J; Thibaut HJ; Strating J; van Kuppeveld FJM The life cycle of non-polio enteroviruses and how to target it. Nat. Rev. Microbiol 2018, 16, 368–381. [PubMed: 29626210]

2. Mao Q; Wang Y; Bian L; Xu M; Liang Z EV-A71 vaccine licensure: a first step for multivalent enterovirus vaccine to control HFMD and other severe diseases. Emerg. Microbes Infect 2016, 5, e75. [PubMed: 27436364]

3. Zhu FC; Meng FY; Li JX; Li XL; Mao QY; Tao H; Zhang YT; Yao X; Chu K; Chen QH; Hu YM; Wu X; Liu P; Zhu LY; Gao F; Jin H; Chen YJ; Dong YY; Liang YC; Shi NM; Ge HM; Liu L; Chen SG; Ai X; Zhang ZY; Ji YG; Luo FJ; Chen XQ; Zhang Y; Zhu LW; Liang ZL; Shen XL Efficacy, safety, and immunology of an inactivated alum-adjuvant enterovirus 71 vaccine in children in China: a multicentre, randomised, double-blind, placebo-controlled, phase 3 trial. Lancet 2013, 381, 2024–2032. [PubMed: 23726161]

4. Wei M; Meng F; Wang S; Li J; Zhang Y; Mao Q; Hu Y; Liu P; Shi N; Tao H; Chu K; Wang Y; Liang Z; Li X; Zhu F 2-Year efficacy, immunogenicity, and safety of vigoo enterovirus 71 vaccine in healthy chinese children: a randomized open-label study. J. Infect. Dis 2017, 215, 56–63. [PubMed: 28077584]

5. Lin JY; Kung YA; Shih SR Antivirals and vaccines for Enterovirus A71. J. Biomed. Sci 2019, 26, 65. [PubMed: 31481071]

6. Lim ZQ; Ng QY; Ng JWQ; Mahendran V; Alonso S Recent progress and challenges in drug development to fight hand, foot and mouth disease. Expert Opin. Drug Discov 2020, 15, 359–371. [PubMed: 31470744]

7. Hu Y; Musharrafieh R; Zheng M; Wang J Enterovirus D68 Antivirals: Past, Present, and Future. ACS Infect. Dis 2020, 6, 1572–1586. [PubMed: 32352280]

8. Bauer L; Lyoo H; van der Schaar HM; Strating JR; van Kuppeveld FJ Direct-acting antivirals and host-targeting strategies to combat enterovirus infections. Curr. Opin. Virol 2017, 24, 1–8. [PubMed: 28411509]

9. Chen B-S; Lee H-C; Lee K-M; Gong Y-N; Shih S-R Enterovirus and Encephalitis. Front. Microbiol 2020, 11, 261. [PubMed: 32153545]

10. Park SW; Pons-Salort M; Messacar K; Cook C; Meyers L; Farrar J; Grenfell BT Epidemiological dynamics of enterovirus D68 in the United States and implications for acute flaccid myelitis. Sci. Transl. Med 2021, 13, eabd2400. [PubMed: 33692131]

11. Pons-Salort M; Oberste MS; Pallansch MA; Abedi GR; Takahashi S; Grenfell BT; Grassly NC The seasonality of nonpolio enteroviruses in the United States: Patterns and drivers. Proc. Natl. Acad. Sci. U S A 2018, 115, 3078–3083. [PubMed: 29507246]

12. Sun J; Hu XY; Yu XF Current understanding of human Enterovirus D68. Viruses 2019, 11, 490.

13. Messacar K; Asturias EJ; Hixon AM; Van Leer-Buter C; Niesters HGM; Tyler KL; Abzug MJ; Dominguez SR Enterovirus D68 and acute flaccid myelitis-evaluating the evidence for causality. Lancet Infect. Dis 2018, 18, e239–e247. [PubMed: 29482893]

14. Brown DM; Hixon AM; Oldfield LM; Zhang Y; Novotny M; Wang W; Das SR; Shabman RS; Tyler KL; Scheuermann RH Contemporary circulating Enterovirus D68 strains have acquired the capacity for viral entry and replication in human neuronal cells. mBio 2018, 9, e01954–18. [PubMed: 30327438]

15. Morens DM; Folkers GK; Fauci AS Acute flaccid myelitis: something old and something new. mBio 2019, 10, e00521–19. [PubMed: 30940708]

16. Murphy OC; Pardo CA Acute flaccid myelitis: a clinical review. Semin. Neurol 2020, 40, 211–218. [PubMed: 32143233]

17. Dyda A; Stelzer-Braid S; Adam D; Chughtai AA; MacIntyre CR The association between acute flaccid myelitis (AFM) and Enterovirus D68 (EV-D68) - what is the evidence for causation? Euro. Surveill 2018, 23, 16–24.

18. Hixon AM; Frost J; Rudy MJ; Messacar K; Clarke P; Tyler KL Understanding Enterovirus D68-induced neurologic disease: a basic science review. Viruses 2019, 11, 821.

19. Messacar K; Sillau S; Hopkins SE; Otten C; Wilson-Murphy M; Wong B; Santoro JD; Treister A; Bains HK; Torres A; Zabrocki L; Glanternik JR; Hurst AL; Martin JA; Schreiner T; Makhani N; DeBiasi RL; Kruer MC; Tremoulet AH; Van Haren K; Desai J; Benson LA; Gorman MP; Abzug MJ; Tyler KL; Dominguez SR Safety, tolerability, and efficacy of fluoxetine as an antiviral for acute flaccid myelitis. Neurology 2019, 92, e2118–e2126. [PubMed: 30413631]

20. Hixon AM; Clarke P; Tyler KL Evaluating treatment efficacy in a mouse model of Enterovirus D68-associated paralytic myelitis. J. Infect. Dis 2017, 216, 1245–1253. [PubMed: 28968718]

21. Hixon AM; Yu G; Leser JS; Yagi S; Clarke P; Chiu CY; Tyler KL A mouse model of paralytic myelitis caused by enterovirus D68. PLoS Pathog. 2017, 13, e1006199. [PubMed: 28231269]

22. Hurst BL; Evans WJ; Smee DF; Van Wettere AJ; Tarbet EB Evaluation of antiviral therapies in respiratory and neurological disease models of Enterovirus D68 infection in mice. Virology 2019, 526, 146–154. [PubMed: 30390563]

23. Morrey JD; Wang H; Hurst BL; Zukor K; Siddharthan V; Van Wettere AJ; Sinex DG; Tarbet EB Causation of acute flaccid paralysis by myelitis and myositis in Enterovirus-D68 infected mice deficient in interferon alphabeta/gamma receptor deficient mice. Viruses 2018, 10, 33.

24. Bowers JR; Valentine M; Harrison V; Fofanov VY; Gillece J; Delisle J; Patton B; Schupp J; Sheridan K; Lemmer D; Ostdiek S; Bains HK; Heim J; Sylvester T; Prasai S; Kretschmer M; Fowle N; Komatsu K; Brady S; Robinson S; Fitzpatrick K; Ostovar GA; Alsop E; Hutchins E; Jensen K; Keim P; Engelthaler DM Genomic analyses of acute flaccid myelitis cases among a cluster in Arizona provide further evidence of Enterovirus D68 role. mBio 2019, 10, e02262–18.

25. Mishra N; Ng TFF; Marine RL; Jain K; Ng J; Thakkar R; Caciula A; Price A; Garcia JA; Burns JC; Thakur KT; Hetzler KL; Routh JA; Konopka-Anstadt JL; Nix WA; Tokarz R; Briese T; Oberste MS; Lipkin WI Antibodies to enteroviruses in cerebrospinal fluid of patients with acute flaccid myelitis. mBio 2019, 10, e01903–19. [PubMed: 31409689]

26. Tee HK; Zainol MI; Sam IC; Chan YF Recent advances in the understanding of enterovirus A71 infection: a focus on neuropathogenesis. Expert Rev. Anti. Infect. Ther 2021, 1–15.

27. Uprety P; Graf EH Enterovirus infection and acute flaccid myelitis. Curr. Opin. Virol 2020, 40, 55–60. [PubMed: 32711392]

28. Martino TA; Liu P; Sole MJ Viral infection and the pathogenesis of dilated cardiomyopathy. Circ. Res 1994, 74, 182–8. [PubMed: 8293557]

29. Dunne JL; Richardson SJ; Atkinson MA; Craig ME; Dahl-Jorgensen K; Flodstrom-Tullberg M; Hyoty H; Insel RA; Lernmark A; Lloyd RE; Morgan NG; Pugliese A Rationale for enteroviral vaccination and antiviral therapies in human type 1 diabetes. Diabetologia 2019, 62, 744–753. [PubMed: 30675626]

30. Xing Y; Zuo J; Krogstad P; Jung ME Synthesis and structure-activity relationship (SAR) studies of novel pyrazolopyridine derivatives as inhibitors of enterovirus replication. J. Med. Chem 2018, 61, 1688–1703. [PubMed: 29346733]

31. Ulferts R; de Boer SM; van der Linden L; Bauer L; Lyoo HR; Mate MJ; Lichiere J; Canard B; Lelieveld D; Omta W; Egan D; Coutard B; van Kuppeveld FJ Screening of a library of FDA-approved drugs identifies several enterovirus replication inhibitors that target viral protein 2C. Antimicrob. Agents Chemother 2016, 60, 2627–2638. [PubMed: 26856848]

32. Bauer L; Manganaro R; Zonsics B; Strating J; El Kazzi P; Lorenzo Lopez M; Ulferts R; van Hoey C; Mate MJ; Langer T; Coutard B; Brancale A; van Kuppeveld FJM Fluoxetine inhibits enterovirus replication by targeting the viral 2C protein in a stereospecific manner. ACS Infect. Dis 2019, 5, 1609–1623. [PubMed: 31305993]

33. Musharrafieh R; Zhang J; Tuohy P; Kitamura N; Bellampalli SS; Hu Y; Khanna R; Wang J Discovery of quinoline analogues as potent antivirals against Enterovirus D68 (EV-D68). J. Med. Chem 2019, 62, 4074–4090. [PubMed: 30912944]

34. Musharrafieh R; Kitamura N; Hu Y; Wang J Development of broad-spectrum enterovirus antivirals based on quinoline scaffold. Bioorg. Chem 2020, 101, 103981. [PubMed: 32559580]

35. Zuo J; Kye S; Quinn KK; Cooper P; Damoiseaux R; Krogstad P Discovery of structurally diverse small-molecule compounds with broad antiviral activity against Enteroviruses. Antimicrob. Agents Chemother 2015, 60, 1615–1626. [PubMed: 26711750]

36. Bauer L; Manganaro R; Zonsics B; Hurdiss DL; Zwaagstra M; Donselaar T; Welter NGE; van Kleef R; Lopez ML; Bevilacqua F; Raman T; Ferla S; Bassetto M; Neyts J; Strating J; Westerink RHS; Brancale A; van Kuppeveld FJM Rational design of highly potent broad-spectrum enterovirus inhibitors targeting the nonstructural protein 2C. PLoS Biol. 2020, 18, e3000904. [PubMed: 33156822]

37. Holm-Hansen CC; Midgley SE; Fischer TK Global emergence of enterovirus D68: a systematic review. Lancet Infect. Dis 2016, 16, e64–e75. [PubMed: 26929196]

38. Ma C; Hu Y; Zhang J; Wang J Pharmacological characterization of the mechanism of action of R523062, a promising antiviral for enterovirus D68. ACS Infect. Dis 2020, 6, 2260–2270. [PubMed: 32692536]

39. Ma C; Hu Y; Zhang J; Musharrafieh R; Wang J A novel capsid binding inhibitor displays potent antiviral activity against Enterovirus D68. ACS Infect. Dis 2019, 5, 1952–1962. [PubMed: 31532189]

40. Guan H; Tian J; Zhang C; Qin B; Cui S Crystal structure of a soluble fragment of poliovirus 2CATPase. PLoS Pathog. 2018, 14, e1007304. [PubMed: 30231078]

41. Guan H; Tian J; Qin B; Wojdyla JA; Wang B; Zhao Z; Wang M; Cui S Crystal structure of 2C helicase from enterovirus 71. Sci. Adv 2017, 3, e1602573. [PubMed: 28508043]

42. Wang SH; Wang K; Zhao K; Hua SC; Du J The Structure, function, and mechanisms of action of Enterovirus non-structural protein 2C. Front. Microbiol 2020, 11, 615965. [PubMed: 33381104]

43. Volochnyuk DM; Ryabukhin SV; Plaskon AS; Dmytriv YV; Grygorenko OO; Mykhailiuk PK; Krotko DG; Pushechnikov A; Tolmachev AA Approach to the library of fused pyridine-4-carboxylic acids by Combes-type reaction of acyl pyruvates and electron-rich amino heterocycles. J. Comb. Chem 2010, 12, 510–517. [PubMed: 20459117]

44. Musharrafieh R; Ma C; Zhang J; Hu Y; Diesing JM; Marty MT; Wang J Validating enterovirus D68-2A(pro) as an antiviral drug target and the discovery of telaprevir as a potent D68-2A(pro) inhibitor. J. Virol 2019, 93, e02221–18. [PubMed: 30674624]

45. Hu Y; Meng X; Zhang F; Xiang Y; Wang J The in vitro antiviral activity of lactoferrin against common human coronaviruses and SARS-CoV-2 is mediated by targeting the heparan sulfate co-receptor. Emerg. Microbes Infect 2021, 10, 317–330. [PubMed: 33560940]

46. Hu Y; Ma C; Szeto T; Hurst B; Tarbet B; Wang J Boceprevir, calpain inhibitors II and XII, and GC-376 have broad-spectrum antiviral activity against coronaviruses. ACS Infect. Dis 2021, 7, 586–597. [PubMed: 33645977]

47. Ma C; Wang J Dipyridamole, chloroquine, montelukast sodium, candesartan, oxytetracycline, and atazanavir are not SARS-CoV-2 main protease inhibitors. Proc. Natl. Acad. Sci. U S A 2021, 118, e2024420118. [PubMed: 33568498]

48. Sacco MD; Ma C; Lagarias P; Gao A; Townsend JA; Meng X; Dube P; Zhang X; Hu Y; Kitamura N; Hurst B; Tarbet B; Marty MT; Kolocouris A; Xiang Y; Chen Y; Wang J Structure and inhibition of the SARS-CoV-2 main protease reveal strategy for developing dual inhibitors against M(pro) and cathepsin L. Sci. Adv 2020, 6, eabe0751. [PubMed: 33158912]

49. Hu Y; Zhang J; Musharrafieh RG; Ma C; Hau R; Wang J Discovery of dapivirine, a nonnucleoside HIV-1 reverse transcriptase inhibitor, as a broad-spectrum antiviral against both influenza A and B viruses. Antiviral Res. 2017, 145, 103–113. [PubMed: 28778830]

50. Takeda M; Pekosz A; Shuck K; Pinto LH; Lamb RA Influenza a virus M2 ion channel activity is essential for efficient replication in tissue culture. J. Virol 2002, 76, 1391–1399. [PubMed: 11773413]
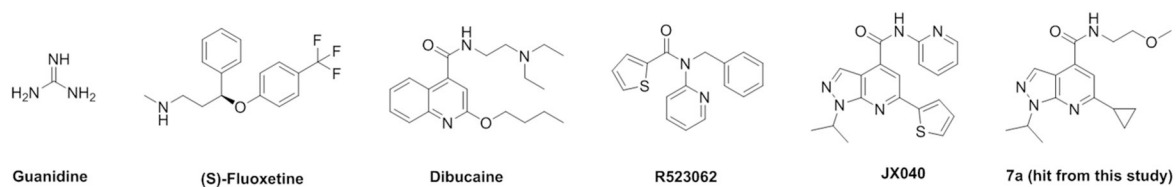
Figure 1.
Structurally diverse enterovirus 2C inhibitors. The hit compound **7a** identified from our high-throughput screening served as a starting point for the lead optimization in this study.

A

B
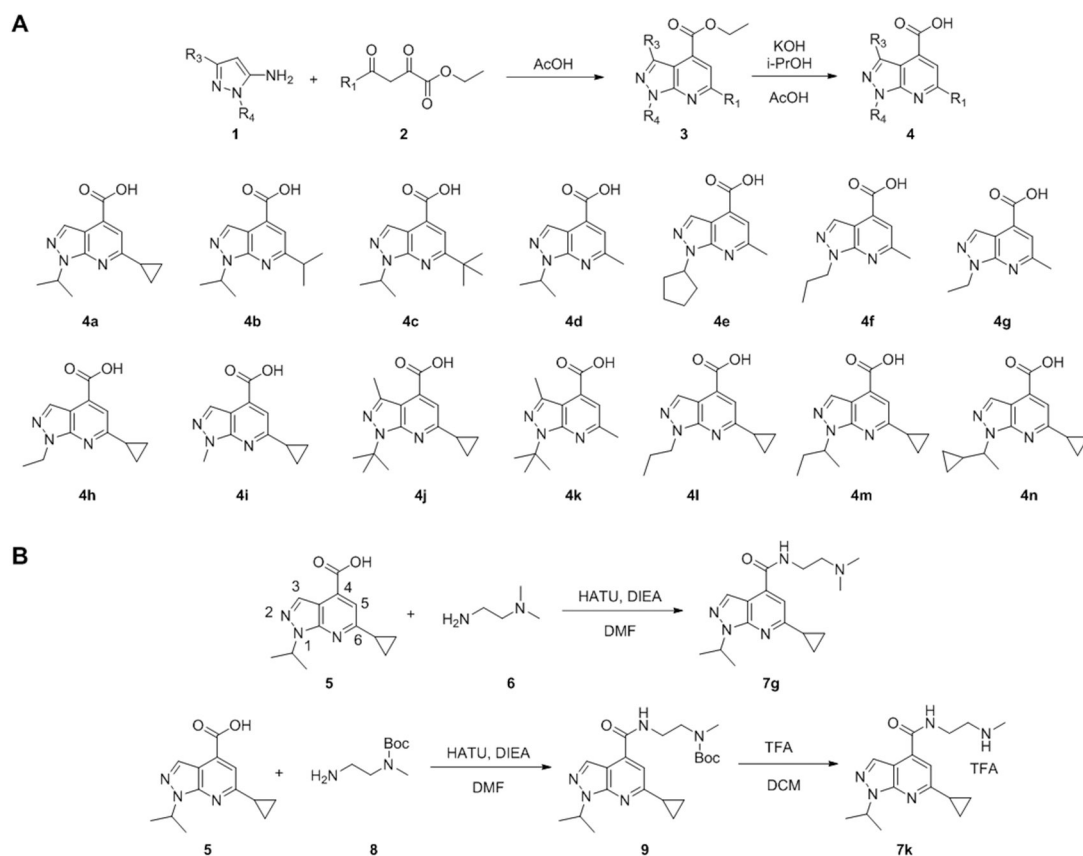
Figure 2.
Synthesis of pyrazolopyridine analogs. (A) Synthesis of 1*H*-pyrazolo[3,4,-*b*]pyridine-4-carboxylic acid. (B) Representative synthesis of pyrazolopyridines with either tertiary amine (**7g**), secondary or primary amine (**7k**).
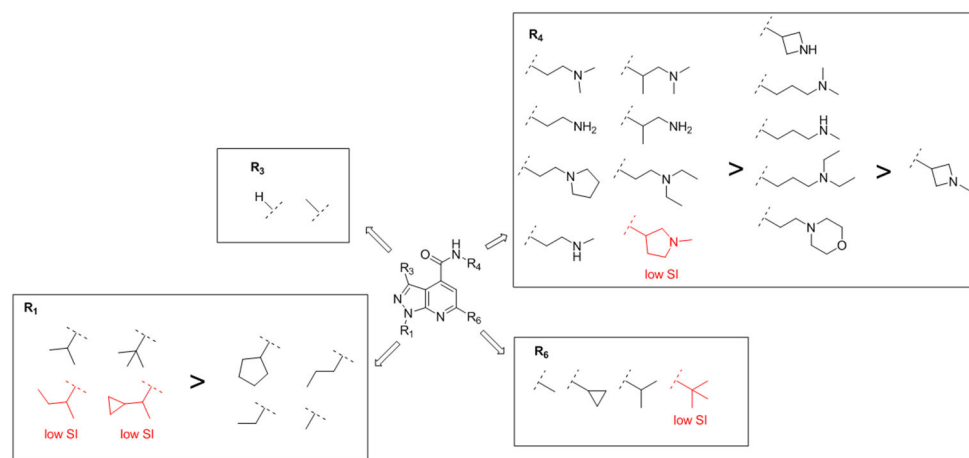
Figure 3.
Summary of SAR studies of pyrazolopyridine. Substitutions led to compounds with a low selectivity index (SI) are labeled in red. Potent leads have each of the shown substituents R_1, R_3, R_4, and R_6.
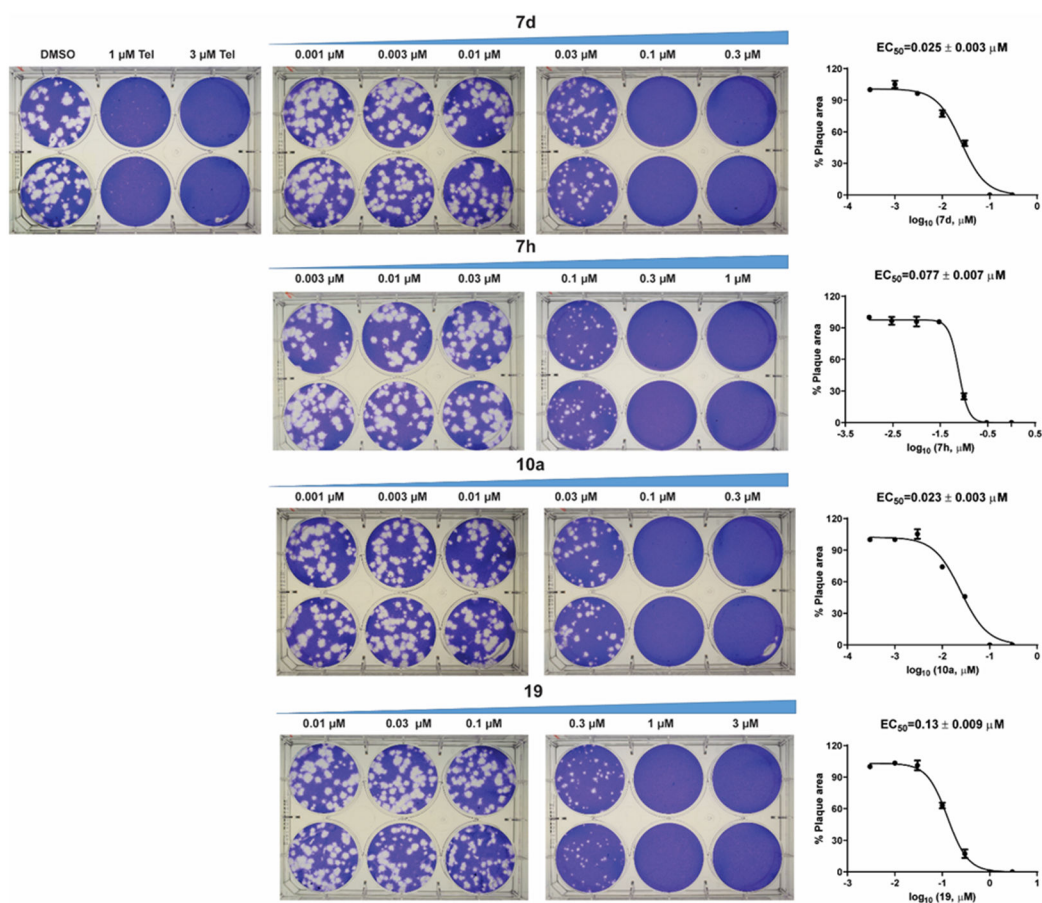
Figure 4.
Antiviral activity of compounds **7d, 7h, 10a**, and **19** against EV-D68 US/MO/14-18947 in plaque assay. The plaque areas were quantified in Image J and EC_{50} values were determined through curve fittings in Graphpad Prism 8 using log(concentration of inhibitors) vs percentage of plaque area with variable slopes. The results are the mean ± standard deviation of two repeats.
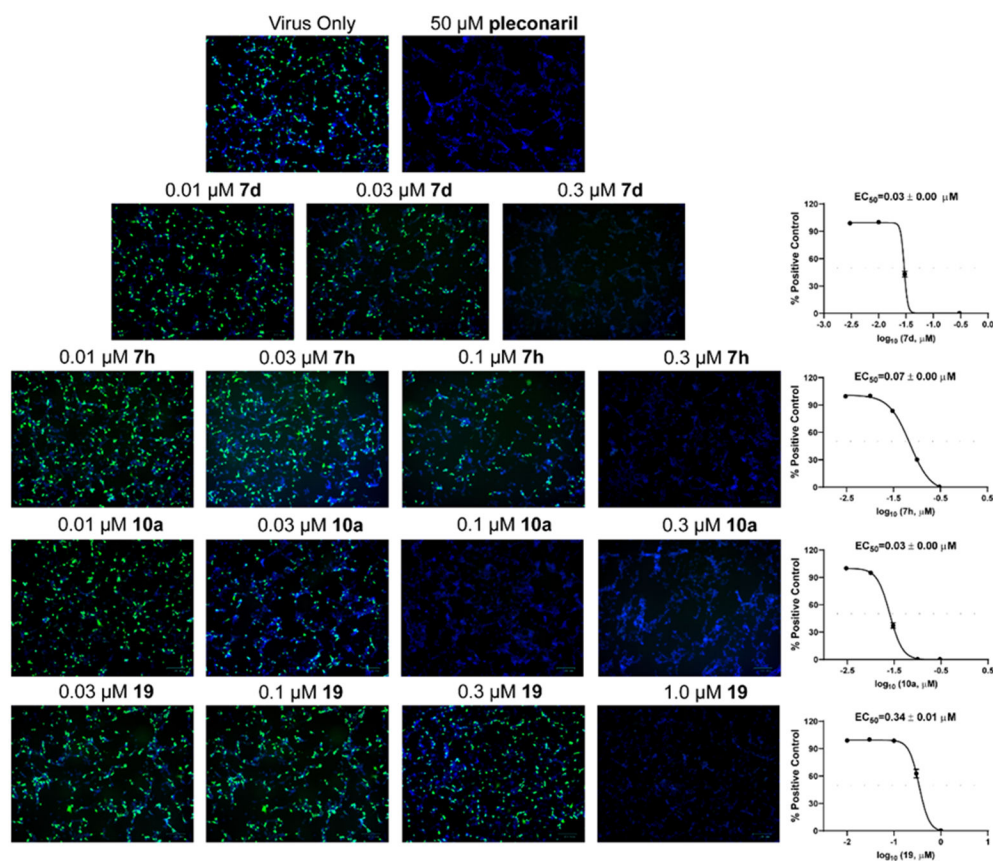
Figure 5.
Antiviral activity of compounds **7d, 7h, 10a**, and **19** against EV-D68 US/MO/14-18947 in neuronal cell line SH-SY5Y using immunofluorescence assay. The immunofluorescence signals were quantified in Image J and EC_{50} values were determined through curve fittings in Graphpad Prism 8 using log(concentration of inhibitors) vs percentage of positive control with variable slopes. The results are the mean ± standard deviation of two repeats.
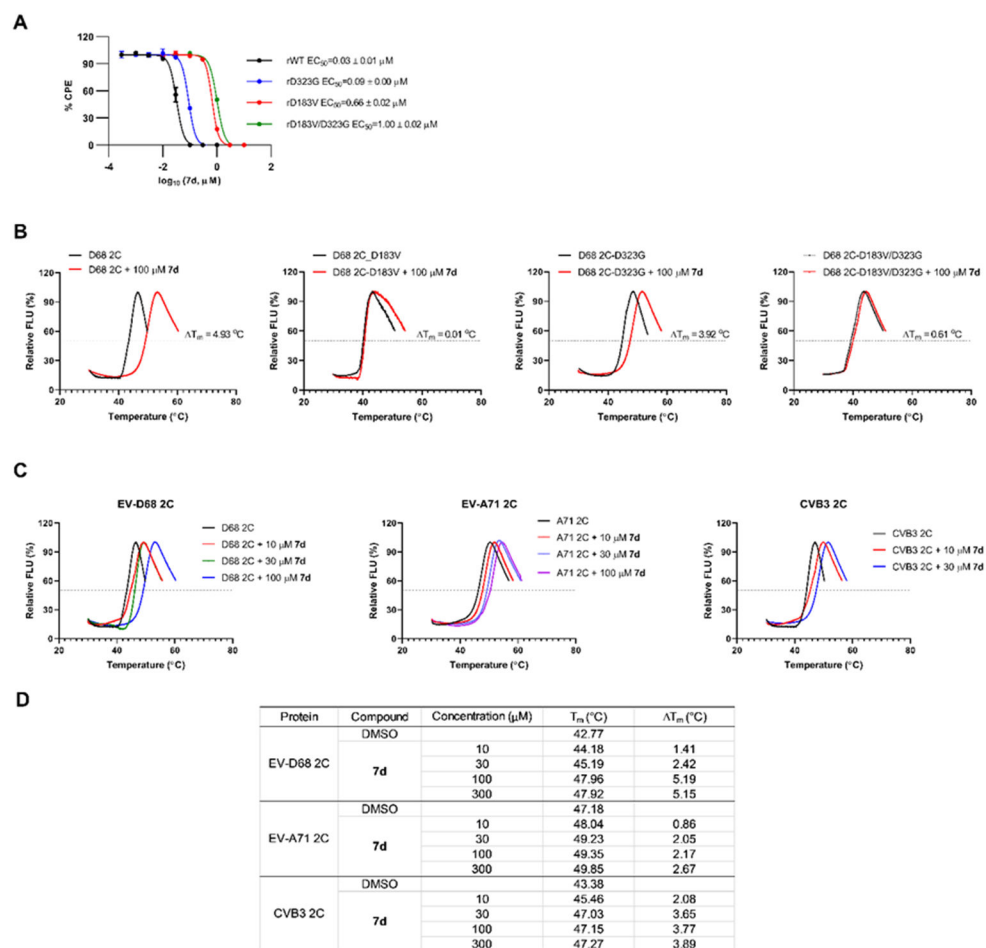
Figure 6.
Mechanism of action of the broad-spectrum antiviral **7d**. (A) Drug sensitivity of **7d** against different strains of recombinant EV-D68 viruses in plaque assay. (B) Thermal shift binding assay of **7d** against purified EV-D68 2C protein and the mutants selected from viral passage experiments. (C) Thermal shift binding assay of **7d** against EV-D68 2C, EV-A71 2C, and CVB3 2C. (D) Melting temperature T_m and thermal shift T_m of EV-D68 2C, EV-A71 2C and CVB3 2C in the presence of different concentrations of **7d**.
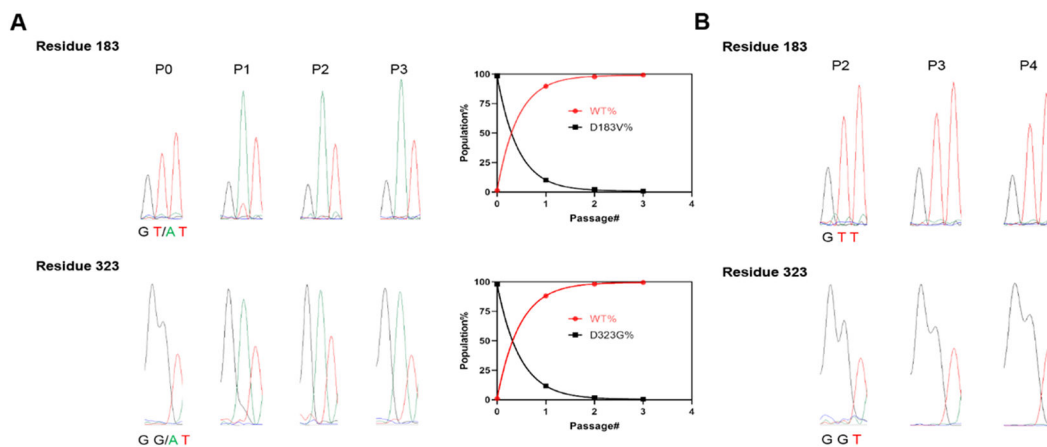
Figure 7.
(A) Competition growth assay of rD183V/D323G with rWT EV-D68 virus. Electropherogram traces of 2C protein coding region were exported from Chromas Lite 2.6, and residues 183 and 323 from viruses at each passage were shown on 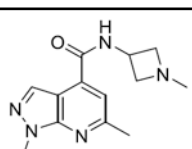the left. Codon GAT is for Asp, condon GTT is for Val, codon GGT is for Gly. The percentages of the mutant and WT virus populations at both positions were determined by measuring the height of the nucleotide peaks in the sequencing trace and shown on the right. (B) Stability of recombinant virus rD183V/D323G propagated in cell culture. The recombinant virus rD183V/D323G was propagated in RD cells sequentially for four passages, and 2C protein coding region from the viruses collected from Passage 2, 3, and 4 (P2, P3, P4) were sequenced. Electropherogram traces at residues 183 and 323 from viruses at each passage were shown.
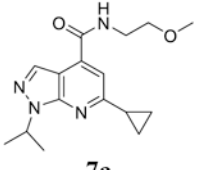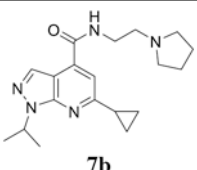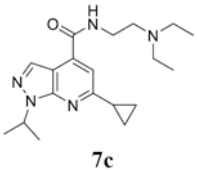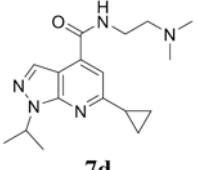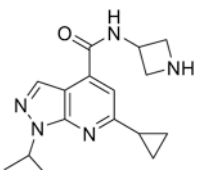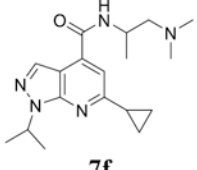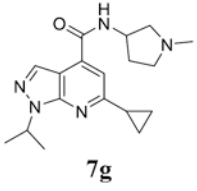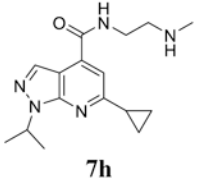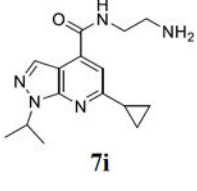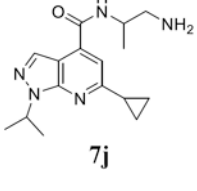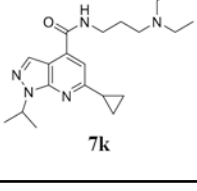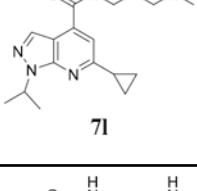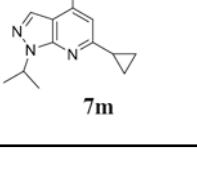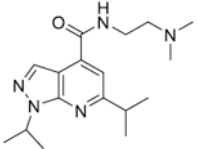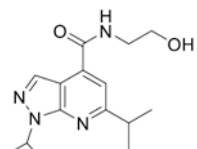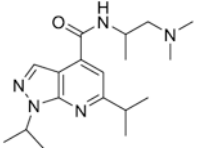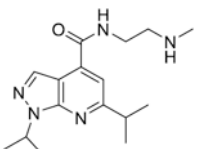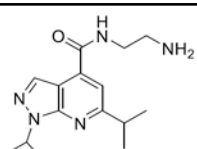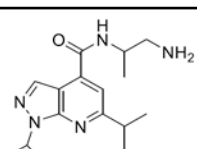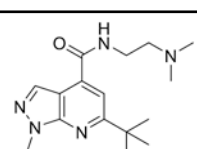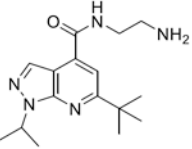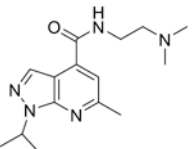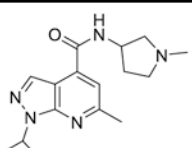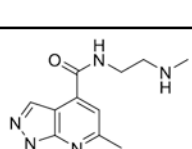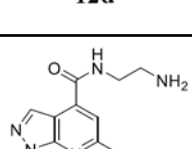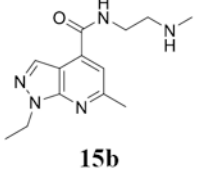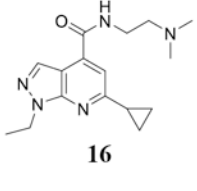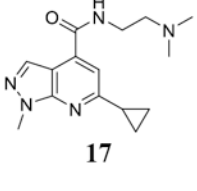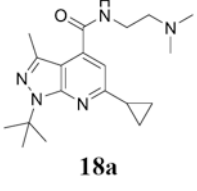
Table 1.
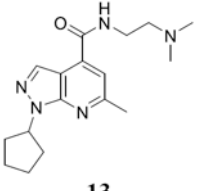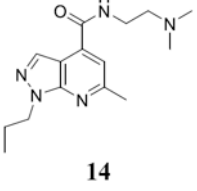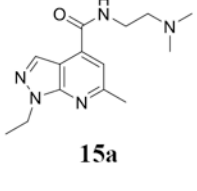
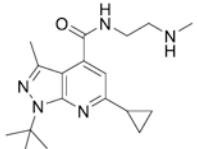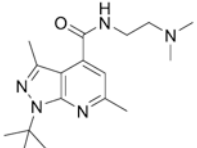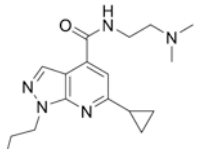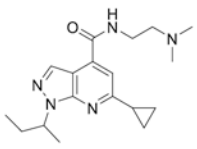SAR study of pyrazolopyridine analogs against EV-D68, EV-A71 and CVB3.

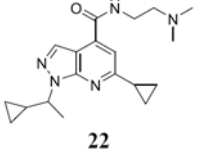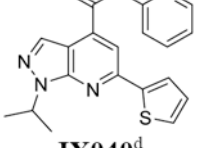| Structure	Anti-EV-D68 US/KY/14-18953 in RD cells (µM)	Anti-EV-A71 Tainan/4643/1998 in RD cells (µM)	Anti-CVB3 in Vero cells (µM)
7a	$EC_{50} = 16.7 \pm 3.8$ $CC_{50} = 177.7 \pm 11.5$ $SI_{50} = 10.6$	$EC_{50} = 8.1 \pm 0.7$ $CC_{50} = 177.7 \pm 11.5$ $SI_{50} = 21.9$	N.T.
7b	$EC_{50} = 0.04 \pm 0.001$ $CC_{50} = 46.5 \pm 3.0$ $SI_{50} = 1162.5$	$EC_{50} = 0.2 \pm 0.1$ $CC_{50} = 46.5 \pm 3.0$ $SI_{50} = 232.5$	$EC_{50} = 0.2 \pm 0.1$ $CC_{50} = 63.1 \pm 8.4$ $SI_{50} = 315.5$
7c	$EC_{50} = 0.4 \pm 0.2$ $CC_{50} = 89.9 \pm 10.8$ $SI_{50} = 224.8$	$EC_{50} = 0.3 \pm 0.2$ $CC_{50} = 89.9$ $SI_{50} = 299.7$	$EC_{50} = 0.5 \pm 0.1$ $CC_{50} = 53.6 \pm 9.3$ $SI_{50} = 107.2$
7d	$EC_{50} = 0.1 \pm 0.03$ $CC_{50} = 200.0 \pm 10.8$ $SI_{50} = 2000.0$	$EC_{50} = 0.8 \pm 0.2$ $CC_{50} = 200.0 \pm 10.8$ $SI_{50} = 250.0$	$EC_{50} = 0.2 \pm 0.1$ $CC_{50} = 125.3 \pm 18.5$ $SI_{50} = 626.5$
7e	$EC_{50} = 1.4 \pm 0.1$ $CC_{50} = 91.6 \pm 22.1$ $SI_{50} = 65.4$	N.T.	N.T.
7f	$EC_{50} = 0.02 \pm 0.001$ $CC_{50} = 72.6 \pm 11.3$ $SI_{50} = 3630.0$	$EC_{50} = 0.1 \pm 0.02$ $CC_{50} = 72.6 \pm 11.3$ $SI_{50} = 726.0$	$EC_{50} = 0.04 \pm 0.002$ $CC_{50} > 300.0$ $SI_{50} > 7500.0$

Structure	Anti-EV-D68 US/KY/14-18953 in RD cells (μM)	Anti-EV-A71 Tainan/4643/1998 in RD cells (μM)	Anti-CVB3 in Vero cells (μM)
7g	$EC_{50} = 0.02 \pm 0.008$ $CC_{50} = 20.7 \pm 1.9$ $SI_{50} = 1035.0$	$EC_{50} = 0.1 \pm 0.05$ $CC_{50} = 20.7 \pm 1.9$ $SI_{50} = 207.0$	$EC_{50} = 0.1 \pm 0.04$ $CC_{50} = 33.8 \pm 2.2$ $SI_{50} = 338.0$
7h	$EC_{50} = 0.2 \pm 0.1$ $CC_{50} = 236.3 \pm 20.5$ $SI_{50} = 1183.0$	$EC_{50} = 0.2 \pm 0.1$ $CC_{50} = 236.3 \pm 20.5$ $SI_{50} = 1183.0$	$EC_{50} = 0.2 \pm 0.1$ $CC_{50} > 100.0$ $SI_{50} > 500.0$
7i	$EC_{50} = 0.4 \pm 0.2$ $CC_{50} = 259.3 \pm 11.3$ $SI_{50} = 648.3$	$EC_{50} = 0.4 \pm 0.1$ $CC_{50} = 259.3 \pm 11.3$ $SI_{50} = 648.3$	$EC_{50} = 0.9 \pm 0.2$ $CC_{50} = 173.8 \pm 11.3$ $SI_{50} = 193.1$
7j	$EC_{50} = 0.3 \pm 0.1$ $CC_{50} = 112.9 \pm 8.7$ $SI_{50} = 376.3$	$EC_{50} = 0.6 \pm 0.1$ $CC_{50} = 112.9 \pm 8.7$ $SI_{50} = 188.2$	$EC_{50} = 0.3 \pm 0.1$ $CC_{50} = 164.2 \pm 8.2$ $SI_{50} = 547.3$
7k	$EC_{50} = 1.9 \pm 0.2$ $CC_{50} = 43.8 \pm 1.3$ $SI_{50} = 23.1$	$EC_{50} = 6.1 \pm 0.5$ $CC_{50} = 43.8 \pm 1.3$ $SI_{50} = 7.2$	$EC_{50} = 1.7 \pm 0.3$ $CC_{50} = 130.2 \pm 6.4$ $SI_{50} = 76.6$
7l	$EC_{50} = 1.2 \pm 0.3$ $CC_{50} = 74.1 \pm 2.5$ $SI_{50} = 61.8$	$EC_{50} = 1.8 \pm 0.4$ $CC_{50} = 74.1 \pm 2.5$ $SI_{50} = 41.2$	$EC_{50} = 0.4 \pm 0.2$ $CC_{50} > 200$ $SI_{50} > 500$
7m	$EC_{50} = 1.7 \pm 0.2$ $CC_{50} = 183.0 \pm 20.1$ $SI_{50} = 107.6$	$EC_{50} = 5.3 \pm 0.2$ $CC_{50} = 183.0 \pm 20.1$ $SI_{50} = 34.5$	$EC_{50} = 1.6 \pm 0.3$ $CC_{50} = 281.3$ $SI_{50} = 175.8$

Structure	Anti-EV-D68 US/KY/14-18953 in RD cells (µM)	Anti-EV-A71 Tainan/4643/1998 in RD cells (µM)	Anti-CVB3 in Vero cells (µM)
10a	$EC_{50} = 0.03 \pm 0.001$ $CC_{50} = 160.9 \pm 12.8$ $SI_{50} = 5363.3$	$EC_{50} = 0.1 \pm 0.03$ $CC_{50} = 160.9 \pm 12.8$ $SI_{50} = 1609.0$	$EC_{50} = 0.04 \pm 0.02$ $CC_{50} > 300.0$ $SI_{50} > 7500.0$
10b	$EC_{50} = 9.8 \pm 2.3$ $CC_{50} > 100.0$ $SI_{50} > 10.2$	N.T.	N.T.
10c	$EC_{50} = 0.1 \pm 0.04$ $CC_{50} > 100.0$ $SI_{50} > 1000.0$	$EC_{50} = 1.0 \pm 0.4$ $CC_{50} = 70.3 \pm 1.9$ $SI_{50} = 703.0$	$EC_{50} = 0.1 \pm 0.04$ $CC_{50} = 116.6 \pm 27.8$ $SI_{50} = 1166.0$
10d	$EC_{50} = 0.4 \pm 0.2$ $CC_{50} > 100.0$ $SI_{50} > 250.0$	$EC_{50} = 0.1 \pm 0.02$ $CC_{50} > 100.0$ $SI_{50} > 1000.0$	$EC_{50} = 0.3 \pm 0.1$ $CC_{50} = 132.9 \pm 27.9$ $SI_{50} = 443.0$
10e	$EC_{50} = 0.6 \pm 0.2$ $CC_{50} = 169.5 \pm 8.6$ $SI_{50} = 282.5$	$EC_{50} = 0.6 \pm 0.2$ $CC_{50} = 169.5 \pm 8.6$ $SI_{50} = 282.5$	$EC_{50} = 0.9 \pm 0.1$ $CC_{50} = 108.1 \pm 22.7$ $SI_{50} = 120.1$
10f	$EC_{50} = 0.2 \pm 0.004$ $CC_{50} = 118.1 \pm 15.4$ $SI_{50} = 590.5$	$EC_{50} = 0.5 \pm 0.3$ $CC_{50} = 118.1 \pm 15.4$ $SI_{50} = 236.2$	$EC_{50} = 0.6 \pm 0.3$ $CC_{50} = 134.8 \pm 5.9$ $SI_{50} = 224.7$
11a	$EC_{50} = 0.1 \pm 0.04$ $CC_{50} = 31.4 \pm 7.1$ $SI_{50} = 314.0$	$EC_{50} = 0.04 \pm 0.003$ $CC_{50} = 31.4 \pm 7.1$ $SI_{50} = 785.0$	$EC_{50} = 0.1 \pm 0.06$ $CC_{50} = 34.4 \pm 2.2$ $SI_{50} = 344.0$

Structure	Anti-EV-D68 US/KY/14-18953 in RD cells (μM)	Anti-EV-A71 Tainan/4643/1998 in RD cells (μM)	Anti-CVB3 in Vero cells (μM)
11b	$EC_{50} = 0.04 \pm 0.002$ $CC_{50} = 24.6 \pm 3.1$ $SI_{50} = 615.0$	$EC_{50} = 0.2 \pm 0.1$ $CC_{50} = 24.6 \pm 3.1$ $SI_{50} = 123.0$	$EC_{50} = 0.1 \pm 0.05$ $CC_{50} = 23.0 \pm 1.5$ $SI_{50} = 230.0$
12a	$EC_{50} = 0.4 \pm 0.2$ $CC_{50} = 112.3 \pm 19.6$ $SI_{50} = 280.8$	$EC_{50} = 0.1 \pm 0.04$ $CC_{50} = 112.3 \pm 19.6$ $SI_{50} = 1123.0$	$EC_{50} = 0.2 \pm 0.03$ $CC_{50} > 300.0$ $SI_{50} > 1500.0$
12b	$EC_{50} = 1.8 \pm 0.2$ $CC_{50} > 300.0$ $SI_{50} > 166.7$	$EC_{50} = 0.5 \pm 0.3$ $CC_{50} > 300.0$ $SI_{50} > 600.0$	$EC_{50} = 0.8 \pm 0.2$ $CC_{50} > 300.0$ $SI_{50} > 375.0$
12c	$EC_{50} = 11.3 \pm 1.6$ $CC_{50} > 300.0$ $SI_{50} > 26.5$	$EC_{50} = 7.3 \pm 0.3$ $CC_{50} > 300.0$ $SI_{50} > 41.1$	$EC_{50} = 3.8 \pm 1.2$ $CC_{50} > 300.0$ $SI_{50} > 78.9$
12d	$EC_{50} = 2.3 \pm 0.2$ $CC_{50} > 300.0$ $SI_{50} > 130.4$	$EC_{50} = 0.5 \pm 0.1$ $CC_{50} > 300.0$ $SI_{50} > 600.0$	$EC_{50} = 1.4 \pm 0.4$ $CC_{50} > 300.0$ $SI_{50} > 214.3$
12e	$EC_{50} = 4.7 \pm 0.6$ $CC_{50} > 300.0$ $SI_{50} > 63.8$	$EC_{50} = 0.7 \pm 0.1$ $CC_{50} > 300.0$ $SI_{50} > 428.6$	$EC_{50} = 3.8 \pm 2.4$ $CC_{50} > 300.0$ $SI_{50} > 78.9$

Structure	Anti-EV-D68 US/KY/14-18953 in RD cells (µM)	Anti-EV-A71 Tainan/4643/1998 in RD cells (µM)	Anti-CVB3 in Vero cells (µM)
13	$EC_{50} = 11.1 \pm 0.3$ $CC_{50} = 88.4 \pm 18.5$ $SI_{50} = 8.0$	N.T.	N.T.
14	$EC_{50} = 48.4 \pm 2.2$ $CC_{50} = 218.6 \pm 25.3$ $SI_{50} = 4.5$	N.T.	N.T.
15a	$EC_{50} = 18.3 \pm 0.5$ $CC_{50} > 300$ $SI_{50} > 16.4$	N.T.	N.T.
15b	$EC_{50} = 58.4 \pm 1.9$ $CC_{50} > 300$ $SI_{50} > 5.1$	$EC_{50} > 20 \ \mu M$	N.T.
16	$EC_{50} = 1.7 \pm 0.2$ $CC_{50} = 263.2 \pm 21.1$ $SI_{50} = 154.8$	$EC_{50} = 1.2 \pm 0.3$ $CC_{50} = 263.2 \pm 21.1$ $SI_{50} = 219.3$	$EC_{50} = 1.8 \pm 0.4$ $CC_{50} > 300$ $SI_{50} > 166.7$
17	$EC_{50} = 9.8 \pm 1.5$ $CC_{50} > 300$ $SI_{50} > 30.6$	N.T.	N.T.
18a	$EC_{50} = 0.8 \pm 0.2$ $CC_{50} = 45.2 \pm 27.6$ $SI_{50} = 56.5$	$EC_{50} = 3.5 \pm 1.2$ $CC_{50} = 45.2 \pm 27.6$ $SI_{50} = 12.9$	$EC_{50} = 1.8 \pm 0.4$ $CC_{50} = 56.3 \pm 11.2$ $SI_{50} = 31.3$

Structure	Anti-EV-D68 US/KY/14-18953 in RD cells (µM)	Anti-EV-A71 Tainan/4643/1998 in RD cells (µM)	Anti-CVB3 in Vero cells (µM)
18b	$EC_{50} = 1.1 \pm 0.5$ $CC_{50} = 31.9 \pm 8.2$ $SI_{50} = 29.0$	$EC_{50} = 8.4 \pm 0.2$ $CC_{50} = 31.9 \pm 8.2$ $SI_{50} = 3.8$	$EC_{50} = 2.9 \pm 0.3$ $CC_{50} = 36.8 \pm 17.8$ $SI_{50} = 12.7$
19	$EC_{50} = 1.0 \pm 0.1$ $CC_{50} = 116.6 \pm 16.1$ $SI_{50} = 116.6$	$EC_{50} = 7.4 \pm 1.7$ $CC_{50} = 116.6 \pm 16.1$ $SI_{50} = 15.8$	$EC_{50} = 2.1 \pm 0.9$ $CC_{50} = 184.0 \pm 13.2$ $SI_{50} = 88.9$
20	$EC_{50} = 1.2 \pm 0.2$ $CC_{50} = 57.7 \pm 10.1$ $SI_{50} = 48.1$	$EC_{50} = 2.0 \pm 0.6$ $CC_{50} = 57.7 \pm 10.1$ $SI_{50} = 28.9$	$EC_{50} = 2.0 \pm 0.3$ $CC_{50} = 111.0 \pm 6.8$ $SI_{50} = 55.5$
21	$EC_{50} = 0.2 \pm 0.1$ $CC_{50} = 40.7 \pm 2.8$ $SI_{50} = 203.5$	$EC_{50} = 0.1 \pm 0.02$ $CC_{50} = 40.7 \pm 2.8$ $SI_{50} = 407.0$	$EC_{50} = 0.1 \pm 0.03$ $CC_{50} = 101.4 \pm 13.6$ $SI_{50} = 1014.0$
22	$EC_{50} = 0.7 \pm 0.2$ $CC_{50} = 28.4 \pm 2.3$ $SI_{50} = 40.6$	$EC_{50} = 0.2 \pm 0.1$ $CC_{50} = 28.4 \pm 2.3$ $SI_{50} = 142.0$	$EC_{50} = 1.9 \pm 0.4$ $CC_{50} = 51.7 \pm 8.3$ $SI_{50} = 27.2$
JX040[d]	$EC_{50} = 0.2 \pm 0.03$ $CC_{50} > 50$ $SI_{50} > 250.0$	N.T.	N.T.

[a] Antiviral potency was determined in the CPE assay with EV-D68 US/KY/14-18953 virus and EV-A71 Tainan/4643/1998 virus in RD cells. For antiviral assay with CVB3 virus Vero cells were used.
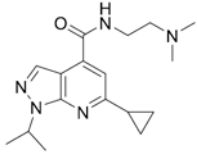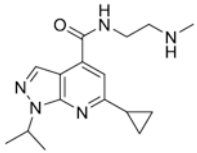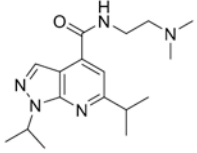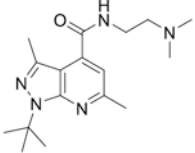
[b] Cytotoxicity was determined using the neutral red uptake method.

[c] N.T.= not tested. The results are the mean ± standard deviation of three repeats. SI = selectivity index (CC_{50}/EC_{50}).

[d] **JX040** also inhibited the EV-D68 US/MO/14-18947 strain with an EC_{50} of 0.1 ± 0.04 µM.

Table 2.

Antiviral activity of potent leads against different serotypes of EV-D68 and EV-A71 in RD cells

EV-strains		7d (μM)	7h (μM)	10a (μM)	19 (μM)
EV-D68	US/KY/14-18953 (Clade D)	EC$_{50}$ = 0.1 ± 0.03 CC$_{50}$ = 200.0 ± 10.8 SI$_{50}$ = 2000	EC$_{50}$ = 0.2 ± 0.1 CC$_{50}$ = 236.3 ± 20.5 SI$_{50}$ = 1183	EC$_{50}$ = 0.03 ± 0.001 CC$_{50}$ = 160.9 ± 12.8 SI$_{50}$ = 5363.3	EC$_{50}$ = 1.0 ± 0.1 CC$_{50}$ = 116.6 ± 16.1 SI$_{50}$ = 116.6
	US/MO/14-18947 (Clade B1)	EC$_{50}$ = 0.1 ± 0.03 CC$_{50}$ = 200.0 ± 10.8 SI$_{50}$ = 2000	EC$_{50}$ = 0.2 ± 0.05 CC$_{50}$ = 236.3 ± 20.5 SI$_{50}$ = 1183	EC$_{50}$ = 0.07 ± 0.01 CC$_{50}$ = 160.9 ± 12.8 SI$_{50}$ = 2298.6	EC$_{50}$ = 0.4 ± 0.2 CC$_{50}$ = 116.6 ± 16.1 SI$_{50}$ = 291.5
	US/MO/14-18949 (Clade B1)	EC$_{50}$ = 0.1 ± 0.02 CC$_{50}$ = 200.0 ± 10.8 SI$_{50}$ = 2000	EC$_{50}$ = 0.2 ± 0.1 CC$_{50}$ = 236.3 ± 20.5 SI$_{50}$ = 1183	EC$_{50}$ = 0.08 ± 0.01 CC$_{50}$ = 160.9 ± 12.8 SI$_{50}$ = 2011.3	EC$_{50}$ = 0.7 ± 0.4 CC$_{50}$ = 116.6 ± 16.1 SI$_{50}$ = 166.6
	US/IL/14-18956 (Clade B2)	EC$_{50}$ = 0.04 ± 0.01 CC$_{50}$ = 200.0 ± 10.8 SI$_{50}$ = 5000	EC$_{50}$ = 0.2 ± 0.04 CC$_{50}$ = 236.3 ± 20.5 SI$_{50}$ = 1183	EC$_{50}$ = 0.07 ± 0.01 CC$_{50}$ = 160.9 ± 12.8 SI$_{50}$ = 2298.6	EC$_{50}$ = 0.4 ± 0.1 CC$_{50}$ = 116.6 ± 16.1 SI$_{50}$ = 291.5
	US/IL/14-18952 (Clade B2)	EC$_{50}$ = 0.04 ± 0.01 CC$_{50}$ = 200.0 ± 10.8 SI$_{50}$ = 5000	EC$_{50}$ = 0.2 ± 0.03 CC$_{50}$ = 236.3 ± 20.5 SI$_{50}$ = 1183	EC$_{50}$ = 0.09 ± 0.01 CC$_{50}$ = 160.9 ± 12.8 SI$_{50}$ = 1787.8	EC$_{50}$ = 0.7 ± 0.02 CC$_{50}$ = 116.6 ± 16.1 SI$_{50}$ = 166.6
EV-A71	Tainan/4643/1998	EC$_{50}$ = 0.1 ± 0.04 CC$_{50}$ = 200.0 ± 10.8 SI$_{50}$ = 2000	EC$_{50}$ = 0.2 ± 0.03 CC$_{50}$ = 236.3 ± 20.5 SI$_{50}$ = 1183	EC$_{50}$ = 0.2 ± 0.04 CC$_{50}$ = 160.9 ± 12.8 SI$_{50}$ = 804.5	EC$_{50}$ = 7.4 ± 1.7 CC$_{50}$ = 236.3 ± 20.5 SI$_{50}$ = 31.9
	USA/CT/2016-19519	EC$_{50}$ = 0.06 ± 0.01 CC$_{50}$ = 200.0 ± 10.8 SI50 = 3333.3	EC$_{50}$ = 0.1 ± 0.04 CC$_{50}$ = 236.3 ± 20.5 SI$_{50}$ = 2363	EC$_{50}$ = 0.06 ± 0.01 CC$_{50}$ = 160.9 ± 12.8 SI$_{50}$ = 2681.7	EC50 = 1.3 ± 0.4 CC50 = 236.3 ± 20.5 SI$_{50}$ = 181.8
	A71 MP4	EC$_{50}$ = 0.1 ± 0.03 CC$_{50}$ = 200.0 ± 10.8 SI$_{50}$ = 2000	EC$_{50}$ = 0.3 ± 0.02 CC$_{50}$ = 236.3 ± 20.5 SI$_{50}$ = 787.7	EC$_{50}$ = 0.2 ± 0.04 CC$_{50}$ = 160.9 ± 12.8 SI$_{50}$ = 804.5	EC$_{50}$ = 2.0 ± 0.3 CC$_{50}$ = 236.3 ± 20.5 SI$_{50}$ = 118.2

[a] Antiviral efficacy EC$_{50}$ was determined using the CPE assay in RD cells.

[b] Cytotoxicity CC$_{50}$ was determined using the neutral red uptake method.

[c] N.T.= not tested. The results are the mean ± standard deviation of three repeats. SI$_{50}$ = selectivity index (CC$_{50}$/EC$_{50}$).

Table 3.

Serial viral passage experiments to select drug resistant mutants against 7d.

Passage #	Drug selection pressure 7d (μM)	Drug sensitivity EC$_{50}$ (μM)	Resistant mutant
P0		0.07 ± 0.02	WT
P1	0.1	N.D.	N.D.
P2	0.1	N.D.	N.D.
P3	0.2	N.D.	N.D.
P4	0.4	N.D.	N.D.
P5	0.8	1.9 ± 0.2	2C protein D183V/D323G

N.D. = not determined.